ON H(div)-CONFORMING METHODS FOR DOUBLE-DIFFUSION EQUATIONS IN POROUS MEDIA*

RAIMUND BÜRGER†, PAUL E. MÉNDEZ†, AND RICARDO RUIZ-BAIER‡

Dedicated to Professor Gabriel N. Gatica on the occasion of his 60th birthday

Abstract. A stationary Navier–Stokes–Brinkman problem coupled to a system of advection-diffusion equations serves as a model for so-called double-diffusive viscous flow in porous media in which both heat and a solute within the fluid phase are subject to transport and diffusion. The solvability analysis of these governing equations results as a combination of compactness arguments and fixed-point theory. In addition an H(div)-conforming discretization is formulated by a modification of existing methods for Brinkman flows. The well-posedness of the discrete Galerkin formulation is also discussed, and convergence properties are derived rigorously. Computational tests confirm the predicted rates of error decay and illustrate the applicability of the methods for the simulation of bacterial bioconvection and thermohaline circulation problems.

Key words. viscous flow in porous media, doubly diffusive problems, cross diffusion, mixed finite element methods, a priori error estimation, fixed-point theory

AMS subject classifications. 65N30, 76S05, 76R50

DOI. 10.1137/18M1196108

1. Introduction.

1.1. Scope. Double-diffusive flows arise in the flow of chemical pollutants in saturated soil, subsurface drilling and petroleum extraction, crystal growth, chemical and food processing, and numerous other applications [10, 22, 23, 30, 46, 36, 39, 41]. This class of models originates in combining heat and mass transfer interacting with flow within porous structures. One of its particularities is the formation of boundary layers due to coupled thermal and compositional mechanisms [14]. This occurs (at least in the case known as augmenting flows) since mass transfer increases the effect of buoyancy due to heat transfer. The difference in the diffusivities of the two fluid components then contributes to redirecting the flow away from the vertical density gradient [42]. Another characteristic phenomenon of double-diffusive flows is cross diffusion [35, 39], where the flux of the solute is influenced by temperature gradients. This so-called Soret effect usually coexists with the reciprocal phenomenon, known as the Dufour effect.

It is the purpose of this work to propose a divergence-conforming finite element method for the doubly-diffusive problem, considering temperature-dependent viscosity and possible cross-diffusion terms subject to the restriction of maintaining the coerciv-

†CI²MA and Departamento de Ingeniería Matemática, Universidad de Concepción, Casilla 160-C, Concepción, Chile (rburger@ing-mat.udec.cl, pmendez@ing-mat.udec.cl).

‡Corresponding author. Mathematical Institute, University of Oxford, Andrew Wiles Building, Woodstock Road, OX2 6GG Oxford, UK (ruizbaier@maths.ox.ac.uk).

ity of the diffusion operator. The formulation includes the Navier–Stokes/Brinkman flow description, which makes this model suitable for the study of flow in saturated porous media and interfaces between porous media and free flow. The numerical scheme is based on $\boldsymbol{H}$(div)-conforming Brezzi–Douglas–Marini (BDM) elements of order k for the velocity, discontinuous elements of order $k-1$ for the pressure, and Lagrangian finite elements of order k for temperature and the concentration of a solute. In particular this formulation produces exactly divergence-free velocity approximations, which are of particular importance in ensuring that solutions to the flow equations remain locally conservative as well as energy stable (see, e.g., [15]) and, moreover, the error estimates of velocity could be derived in a pressure-robust manner (see [26]). Another consequence of local conservation is that the coupled systems (in the present case, of temperature and reactive concentrations) can be written, at the discrete level, in exact divergence form.

The governing equations are posed on an open and bounded spatial domain $\Omega \subseteq \mathbb{R}^d$, $d = 2$ or $d = 3$, with boundary conditions imposed on the boundary $\Gamma = \partial\Omega$ that is assumed to be Lipschitz. The model adopts the form of the incompressible Brinkman–Navier–Stokes equations for the viscous flow of an incompressible Newtonian fluid in a porous medium, where the velocity $\boldsymbol{u}$ and the pressure p are the unknowns, coupled with a pair of advection-diffusion equations with cross diffusion that describe the diffusion of heat and solute. Specifically, we assume that a given species (e.g., salt) has a slight solubility within this fluid, and that S denotes its concentration (i.e., weight of solute per unit weight of solution), while T is temperature, and $\boldsymbol{y} := (T, S)^{\mathrm{T}}$. The stationary behavior of this system can be expressed as follows:

$$
(1.1) \quad \begin{aligned} \boldsymbol{K}^{-1}\boldsymbol{u} + (\boldsymbol{u}\cdot\nabla)\boldsymbol{u} - \mathbf{div}(\nu(T)\nabla\boldsymbol{u}) + \nabla p &= \boldsymbol{F}(\boldsymbol{y}), \quad \mathrm{div}\,\boldsymbol{u} = 0 \quad \text{in } \Omega, \\ -\mathbf{div}(\boldsymbol{D}\nabla\boldsymbol{y}) + \mathrm{div}(\boldsymbol{u}\otimes\boldsymbol{y}) &= 0 \quad \text{in } \Omega, \quad \boldsymbol{y} = \boldsymbol{y}^{\mathrm{D}}, \quad \boldsymbol{u} = \boldsymbol{0} \quad \text{on } \Gamma, \end{aligned}
$$

where $\boldsymbol{K}(\boldsymbol{x}) > 0$ is the permeability matrix rescaled with viscosity, $\boldsymbol{F}(\boldsymbol{y})$ is a given function modeling buoyancy, $\boldsymbol{D}$ is the 2×2 constant matrix of the thermal conductivity and solutal diffusivity coefficients (possibly with cross-diffusion terms), and ν is a temperature-dependent viscosity function. (Precise assumptions on the model functions and problem data are stated in section 2.)

1.2. Related work. To put the paper further into the proper perspective, we mention that in many heat and mass transfer processes, the Soret and Dufour effects can be neglected as their contributions can be orders of magnitude smaller than those described by terms arising from Fourier's or Fick's law. However, these effects can be significant when species are introduced at a surface in a fluid domain and have different densities in comparison to the surrounding fluid. These mechanisms are important as well in applications related to the transport of moisture in fibrous insulations or grain storage insulations and the dispersion of contaminants through water saturated soil, biochemical contaminants transport in environmental problems, and underground disposal of nuclear waste and crystal growth processes [10].

With respect to the well-posedness of (1.1) (under suitable assumptions), we first restrict the discussion to classical Boussinesq-type equations. The solvability of the associated PDEs goes back to Lorca and Boldrini [33, 34]. These works include existence, regularity, and conditions for uniqueness addressing both stationary and nonstationary cases. These results hold for temperature-dependent viscosity and thermal conductivity. Related to the context of our specific problem, the analysis of solutions to doubly-diffusive problems has been addressed, e.g., in [23, 32].

On the other hand, a diversity of numerical methods is available for classical Boussinesq equations as well as for their generalizations to temperature-dependent coefficients. We mention for instance the stabilized finite elements (using projection-based techniques) proposed and rigorously analyzed in [3, 14], the mixed formulations analyzed in [2, 6, 7, 16], and also the stability of splitting schemes (for discontinuous Galerkin, spectral, and vorticity-based finite element formulations) and some more applicative examples have been explored in [1, 5, 13, 30, 31, 36, 40, 41, 44]. Mixed-primal and fully mixed schemes using $\boldsymbol{H}(\mathrm{div})$-conforming velocity approximations have been studied in [37, 38].

The main differences between the available well-posedness results and analysis of $\boldsymbol{H}(\mathrm{div})$-conforming methods for classical Boussinesq equations and the doubly-diffusive equations (1.1) are, of course, caused by the vector-valued nature of the quantities (the components of $\boldsymbol{y}$) that diffuse in (1.1) while in the classical Boussinesq formulation there is only one scalar diffusive quantity (for instance, solely temperature). Some of the arguments related to the well-posedness analysis of the continuous problem, in particular those related to handling nonhomogenous Dirichlet data by a lifting argument [33, 37], carry over almost verbatim from the scalar to the vectorial case. However, the bilinear form associated with the term $-\mathbf{div}(\boldsymbol{D}\nabla\boldsymbol{y})$ must be coercive so that stability is ensured. This requirement, in turn, imposes restrictions on the choice of the diffusion matrix $\boldsymbol{D}$; this matrix must be positive definite (though not necessarily symmetric). These properties are essential for the proof of existence of a discrete solution, as we will elaborate in section 4. In other words, the well-posedness of the variational formulations of (1.1) and the associated $\boldsymbol{H}(\mathrm{div})$-conforming method depend on the proper choice of the entries of $\boldsymbol{D}$.

Other contributions to this area include the finite volume discretizations for thermal and solutal buoyancy within Darcy–Brinkman flows introduced in [22], the error analysis for spectral methods applied to bioconvection in [18], or the vorticity-based Brinkman and nonlinear advection-reaction-diffusion systems analyzed via fixed-point and compactness arguments in [8], that also includes a mixed-primal scheme featuring divergence-free discrete velocities. Penalty Petrov–Galerkin methods were used for the solution of double-diffusion convective problems in [25]. In [42] the authors introduce least-squares schemes specifically tailored for Rayleigh–Bénard convective flows, and the averaging finite element method has been employed in [45] for solidification problems having the same structure as the models we examine here.

1.3. Outline of the paper. The remainder of this paper is organized as follows. In section 2 we introduce some recurrent notation and definitions of functional spaces (section 2.1), specify the assumptions on the model coefficients and problem data and state the problem in variational form (section 2.2), and establish auxiliary properties of the bilinear and trilinear forms involved (section 2.3). Section 3, which follows closely the analysis of [37], is devoted to the well-posedness analysis of the continuous problem (1.1). The basic idea consists in utilizing the correspondence of solutions $(\boldsymbol{u}, p, \boldsymbol{y})$ of the variational formulation of (1.1) with solutions $(\boldsymbol{u}, \boldsymbol{y})$ of a problem in which the pressure does not appear. The main results of section 3 are Theorems 3.1 and 3.2, stating the existence and uniqueness, respectively, of a variational solution of (1.1) under appropriate assumptions. The $\boldsymbol{H}(\mathrm{div})$-conforming method for (1.1) is then introduced and analyzed in section 4, which is at the core of this paper. Specifically, in section 4.1 the method is formulated (based on an appropriate choice of the underlying discrete spaces), and in section 4.2 discrete stability properties of the bilinear and trilinear forms at discrete level are provided. These properties allow us then, in

section 4.3, to establish existence of a discrete solution. This follows from the main result of that section, Theorem 4.1, which is based on a fixed-point argument. Finally, in section 4.4 we conduct an a priori error analysis and, in particular, establish orders of convergence (in terms of the mesh size) of the discrete solution to the continuous one. In section 5 we present results of three different numerical experiments, namely, an accuracy test for a two-dimensional manufactured solution that confirms that the experimentally observed orders of convergence are consistent with those predicted in section 4.4 (Example 1, section 5.1), an illustration of the Soret and Dufour effects in a two-dimensional porous cavity setup that validates the method against benchmark data from literature (Example 2, section 5.2), and simulations of a nonstationary problem on a three-dimensional domain describing bioconvection of oxytactic bacteria that evaluates the extension of the proposed methods to nonlinear cross-diffusion and reaction terms in the diffusion-advection equations.

2. The model problem.

2.1. Preliminaries. Let Ω be an open and bounded domain in $\mathbb{R}^d$, $d = 2, 3$ with Lipschitz boundary $\Gamma = \partial\Omega$. We denote by $L^p(\Omega)$ and $W^{r,p}(\Omega)$ the usual Lebesgue and Sobolev spaces with respective norms $\|\cdot\|_{L^p(\Omega)}$ and $\|\cdot\|_{W^{r,p}(\Omega)}$. If $p = 2$ we write $H^r(\Omega)$ in place of $W^{r,p}(\Omega)$, and denote the corresponding norm by $\|\cdot\|_{r,\Omega}$, ($\|\cdot\|_{0,\Omega}$ for $H^0(\Omega) = L^2(\Omega)$). The space $L_0^2(\Omega)$ denotes the restriction of $L_2(\Omega)$ to functions with zero mean value over Ω. For $r \geq 0$, we write the H^r-seminorm as $|\cdot|_{r,\Omega}$ and we denote by $(\cdot, \cdot)_\Omega$ the usual inner product in $L^2(\Omega)$. Spaces of vector-valued functions (in dimension d) are denoted in bold face, i.e., $\boldsymbol{H}^r(\Omega) = [H^r(\Omega)]^d$, and we use the vector-valued Hilbert spaces

$$\boldsymbol{H}(\mathrm{div}; \Omega) := \big\{ \boldsymbol{w} \in \boldsymbol{L}^2(\Omega) : \mathrm{div}\, \boldsymbol{w} \in L^2(\Omega) \big\},$$

$$\boldsymbol{H}_0(\mathrm{div}; \Omega) := \big\{ \boldsymbol{w} \in \boldsymbol{H}(\mathrm{div}; \Omega) : \boldsymbol{w} \cdot \boldsymbol{n}_{\partial\Omega} = 0 \text{ on } \partial\Omega \big\},$$

$$\boldsymbol{H}_0(\mathrm{div}^0; \Omega) := \big\{ \boldsymbol{w} \in \boldsymbol{H}_0(\mathrm{div}; \Omega) : \mathrm{div}\, \boldsymbol{w} = 0 \text{ in } \Omega \big\},$$

where $\boldsymbol{n}_{\partial\Omega}$ denotes the outward normal on $\partial\Omega$; and we endow these spaces with the norm $\|\boldsymbol{w}\|_{\mathrm{div},\Omega}^2 := \|\boldsymbol{w}\|_{0,\Omega}^2 + \|\mathrm{div}\, \boldsymbol{w}\|_{0,\Omega}^2$.

2.2. Assumptions and weak form of the governing equations. We assume boundary data regularity $\boldsymbol{y}^\mathrm{D} = (T^\mathrm{D}, S^\mathrm{D}) \in [H^{1/2}(\Gamma)]^2$, as well as Lipschitz continuity and uniform boundedness of the kinematic (temperature dependent) viscosity, i.e.,

$$(2.1) \qquad \big|\nu(T_1) - \nu(T_2)\big| \leq \gamma_\nu |T_1 - T_2| \quad \text{and} \quad \nu_1 \leq \nu(T) \leq \nu_2,$$

where γ_ν, ν_1, ν_2 are positive constants. Moreover, we assume Lipschitz continuity of the function $\boldsymbol{F}(\boldsymbol{y})$ defining the buoyancy term, i.e., there exist $\gamma_{\boldsymbol{F}}, C_{\boldsymbol{F}} > 0$ such that

$$(2.2) \qquad \big|\boldsymbol{F}(\boldsymbol{y}_1) - \boldsymbol{F}(\boldsymbol{y}_2)\big| \leq \gamma_{\boldsymbol{F}} |\boldsymbol{y}_1 - \boldsymbol{y}_2| \quad \text{and} \quad \big|\boldsymbol{F}(\boldsymbol{y})\big| \leq C_{\boldsymbol{F}} |\boldsymbol{y}|.$$

The $d \times d$ permeability matrix $\boldsymbol{K}$ is assumed symmetric and uniformly positive definite, hence, its inverse satisfies $\boldsymbol{v}^\mathrm{T} \boldsymbol{K}^{-1}(\boldsymbol{x}) \boldsymbol{v} \geq \alpha_1 |\boldsymbol{v}|^2$ for all $\boldsymbol{v} \in \mathbb{R}^d$ and $\boldsymbol{x} \in \Omega$ for a constant $\alpha_1 > 0$. We also require $\boldsymbol{D}$ to be positive definite, i.e., $\boldsymbol{s}^\mathrm{T} \boldsymbol{D} \boldsymbol{s} \geq \alpha_2 |\boldsymbol{s}|^2$ for all $\boldsymbol{s} \in \mathbb{R}^2$ for a constant $\alpha_2 > 0$.

The variational formulation of problem (1.1) is obtained by testing against suitable functions and integrating by parts, and can be formulated as follows:

Find $(\boldsymbol{u}, p, \boldsymbol{y}) \in \boldsymbol{H}_0^1(\Omega) \times L_0^2(\Omega) \times [H^1(\Omega)]^2$ satisfying $\boldsymbol{y} = \boldsymbol{y}^{\mathrm{D}}$ on Γ and

(2.3)
$$a(\boldsymbol{y}; \boldsymbol{u}, \boldsymbol{v}) + c(\boldsymbol{u}; \boldsymbol{u}, \boldsymbol{v}) + b(\boldsymbol{v}, p) = d(\boldsymbol{y}, \boldsymbol{v}) \quad \text{for all } \boldsymbol{v} \in \boldsymbol{H}_0^1(\Omega),$$
$$b(\boldsymbol{u}, q) = 0 \quad \text{for all } q \in L_0^2(\Omega),$$
$$a_{\boldsymbol{y}}(\boldsymbol{y}, \boldsymbol{s}) + c_{\boldsymbol{y}}(\boldsymbol{u}; \boldsymbol{y}, \boldsymbol{s}) = 0 \quad \text{for all } \boldsymbol{s} \in [H_0^1(\Omega)]^2,$$

where the involved forms are defined as

$$a(\boldsymbol{s}; \boldsymbol{u}, \boldsymbol{v}) := (\boldsymbol{K}^{-1}\boldsymbol{u}, \boldsymbol{v})_\Omega + \big(\nu(\boldsymbol{s})\nabla\boldsymbol{u}, \nabla\boldsymbol{v}\big)_\Omega, \quad c(\boldsymbol{w}; \boldsymbol{u}, \boldsymbol{v}) := \big((\boldsymbol{w}\cdot\nabla)\boldsymbol{u}, \boldsymbol{v}\big)_\Omega,$$
$$b(\boldsymbol{v}, q) := (q, \mathrm{div}\,\boldsymbol{v})_\Omega, \quad d(\boldsymbol{s}, \boldsymbol{v}) := \big(\boldsymbol{F}(\boldsymbol{s}), \boldsymbol{v}\big)_\Omega,$$
$$a_{\boldsymbol{y}}(\boldsymbol{y}, \boldsymbol{s}) := (\boldsymbol{D}\nabla\boldsymbol{y}, \nabla\boldsymbol{s})_\Omega, \quad c_{\boldsymbol{y}}(\boldsymbol{v}; \boldsymbol{y}, \boldsymbol{s}) := \big((\boldsymbol{v}\cdot\nabla)\boldsymbol{y}, \boldsymbol{s}\big)_\Omega$$

for all $\boldsymbol{u}, \boldsymbol{v}, \boldsymbol{w} \in \boldsymbol{H}^1(\Omega)$, $q \in L^2(\Omega)$, and $\boldsymbol{y}, \boldsymbol{s} \in [H^1(\Omega)]^2$, where $\nu(\boldsymbol{s})$ is understood as the kinematic viscosity depending only on the first component of the vector $\boldsymbol{s}$.

2.3. Stability properties. First, note that due to (2.1)–(2.2), the following continuity properties hold for all $\boldsymbol{u}, \boldsymbol{v}, \in \boldsymbol{H}^1(\Omega)$, $q \in L^2(\Omega)$, and $\boldsymbol{y}, \boldsymbol{s} \in [H^1(\Omega)]^2$:

(2.4a)
$$\big|a(\cdot, \boldsymbol{u}, \boldsymbol{v})\big| \le \max\{\nu_2, \|\boldsymbol{K}^{-1}\|_\infty\}\big(\|\nabla\boldsymbol{u}\|_{0,\Omega}\|\nabla\boldsymbol{v}\|_{0,\Omega} + \|\boldsymbol{u}\|_{0,\Omega}\|\boldsymbol{v}\|_{0,\Omega}\big)$$
$$\le C_a\|\boldsymbol{u}\|_{1,\Omega}\|\boldsymbol{v}\|_{1,\Omega},$$

(2.4b) $\big|a_{\boldsymbol{y}}(\boldsymbol{y}, \boldsymbol{s})\big| \le \hat{C}_a\|\boldsymbol{y}\|_{1,\Omega}\|\boldsymbol{s}\|_{1,\Omega},$

(2.4c) $\big|b(\boldsymbol{v}, q)\big| \le \|\boldsymbol{v}\|_{1,\Omega}\|q\|_{0,\Omega},$

(2.4d) $\big|d(\boldsymbol{y}, \boldsymbol{v})\big| \le C_{\boldsymbol{F}}\|\boldsymbol{y}\|_{1,\Omega}\|\boldsymbol{v}\|_{1,\Omega}.$

In addition, and due to the Lipschitz continuity of ν (stated in (2.1)) and Hölder's inequality, the following property holds for all $\boldsymbol{y}_1, \boldsymbol{y}_2 \in [H^1(\Omega)]^2$ and $\boldsymbol{u} \in \boldsymbol{W}^{1,\infty}(\Omega)$:

(2.5)
$$\big|a(\boldsymbol{y}_1; \boldsymbol{u}, \boldsymbol{v}) - a(\boldsymbol{y}_2; \boldsymbol{u}, \boldsymbol{v})\big| \le \gamma_\nu\|\boldsymbol{u}\|_{W^{1,\infty}(\Omega)}\|\boldsymbol{y}_1 - \boldsymbol{y}_2\|_{1,\Omega}\|\boldsymbol{v}\|_{1,\Omega}.$$

On the other hand, standard Sobolev embeddings indicate that for $r \ge 1$ if $d = 2$ or $r \in [1, 6]$ if $d = 3$, there exists $C_r^* > 0$ depending only upon $|\Omega|$ and r such that $\|\boldsymbol{w}\|_{\boldsymbol{L}^r(\Omega)} \le C_r^*\|\boldsymbol{w}\|_{1,\Omega}$ for all $\boldsymbol{w} \in \boldsymbol{H}^1(\Omega)$. Then taking $\boldsymbol{u}, \boldsymbol{v}, \boldsymbol{w} \in \boldsymbol{H}^1(\Omega)$ and $\boldsymbol{y}, \boldsymbol{s} \in [H^1(\Omega)]^2$, and applying this inequality along with Hölder's inequality with $\frac{1}{r} + \frac{1}{r^*} = \frac{1}{2}$, gives the following bounds:

(2.6)
$$\big|c(\boldsymbol{w}; \boldsymbol{u}, \boldsymbol{v})\big| \le C_r^* C_{r^*}^*\|\boldsymbol{w}\|_{1,\Omega}\|\boldsymbol{u}\|_{1,\Omega}\|\boldsymbol{v}\|_{1,\Omega} = C_v\|\boldsymbol{w}\|_{1,\Omega}\|\boldsymbol{u}\|_{1,\Omega}\|\boldsymbol{v}\|_{1,\Omega},$$
$$\big|c_{\boldsymbol{y}}(\boldsymbol{w}; \boldsymbol{y}, \boldsymbol{s})\big| \le C_6^*\|\boldsymbol{w}\|_{1,\Omega}\|\boldsymbol{y}\|_{1,\Omega}\|\boldsymbol{s}\|_{[L^3(\Omega)]^2} = \bar{C}_v\|\boldsymbol{w}\|_{1,\Omega}\|\boldsymbol{y}\|_{1,\Omega}\|\boldsymbol{s}\|_{[L^3(\Omega)]^2},$$
$$\big|c_{\boldsymbol{y}}(\boldsymbol{w}; \boldsymbol{y}, \boldsymbol{s})\big| \le C_6^* C_3^*\|\boldsymbol{w}\|_{1,\Omega}\|\boldsymbol{y}\|_{1,\Omega}\|\boldsymbol{s}\|_{1,\Omega} = \hat{C}_v\|\boldsymbol{w}\|_{1,\Omega}\|\boldsymbol{y}\|_{1,\Omega}\|\boldsymbol{s}\|_{1,\Omega}.$$

Next, Poincaré's inequality together with the properties stated in section 2.2 implies that the bilinear forms $a(\cdot; \cdot, \cdot)$ (for a fixed temperature) and $a_{\boldsymbol{y}}(\cdot, \cdot)$ are coercive, that is,

(2.7a) $a(\cdot; \boldsymbol{v}, \boldsymbol{v}) \ge \min\{\nu_1, \alpha_1\}\big(\|\nabla\boldsymbol{v}\|_{0,\Omega}^2 + \|\boldsymbol{v}\|_{0,\Omega}^2\big) \ge \alpha_a\|\boldsymbol{v}\|_{1,\Omega}^2 \quad \text{for all } \boldsymbol{v} \in \boldsymbol{H}_0^1(\Omega),$

(2.7b) $a_{\boldsymbol{y}}(\boldsymbol{s}, \boldsymbol{s}) \ge \alpha_2|\boldsymbol{s}|_{1,\Omega}^2 \ge \hat{\alpha}_a\|\boldsymbol{s}\|_{1,\Omega}^2 \quad \text{for all } \boldsymbol{s} \in [H_0^1(\Omega)]^2.$

Using the definition and characterization of the kernel $\boldsymbol{X}$ of $b(\cdot,\cdot)$, namely,

$$\boldsymbol{X} := \left\{\boldsymbol{v}\in\boldsymbol{H}_0^1(\Omega) : b(\boldsymbol{v},q)=0 \;\forall q\in L_0^2(\Omega)\right\} = \left\{\boldsymbol{v}\in\boldsymbol{H}_0^1(\Omega) : \operatorname{div}\boldsymbol{v}=0 \text{ in } \Omega\right\},$$

and using integration by parts we can readily observe that

$$(2.8) \quad c(\boldsymbol{w};\boldsymbol{v},\boldsymbol{v})=0 \text{ and } c_{\boldsymbol{y}}(\boldsymbol{w};\boldsymbol{s},\boldsymbol{s})=0 \text{ for all } \boldsymbol{w}\in\boldsymbol{X},\boldsymbol{v}\in\boldsymbol{H}^1(\Omega),\boldsymbol{s}\in[H^1(\Omega)]^2.$$

Remark 1. Note that (2.7a) together with (2.8) implies the $\boldsymbol{H}_0^1(\Omega)$-ellipticity of the bilinear form $a(\boldsymbol{y},\cdot,\cdot)+c(\boldsymbol{w},\cdot,\cdot):\boldsymbol{H}_0^1(\Omega)\times\boldsymbol{H}_0^1(\Omega)\to\mathbb{R}$ for any given $\boldsymbol{y}\in[H^1(\Omega)]^2$ and $\boldsymbol{w}\in\boldsymbol{X}$.

Moreover, the bilinear form $b(\cdot,\cdot)$ satisfies an inf-sup condition:

$$\sup_{\boldsymbol{v}\in\boldsymbol{H}_0^1(\Omega)\setminus\{\boldsymbol{0}\}} \frac{b(\boldsymbol{v},q)}{\|\boldsymbol{v}\|_{1,\Omega}} \geq \beta\|q\|_{0,\Omega} \quad \text{for all } q\in L_0^2(\Omega)$$

(see [43] for this well-known property). Finally, for $\boldsymbol{u}\in\boldsymbol{W}^{1,\infty}(\Omega)$ and $\boldsymbol{s}\in[H^1(\Omega)\cap L^\infty(\Omega)]^2$ there exists an embedding constant $C_\infty>0$ such that

$$(2.9) \qquad \|\boldsymbol{u}\|_{1,\Omega}\leq C_\infty\|\boldsymbol{u}\|_{\boldsymbol{W}^{1,\infty}(\Omega)} \quad \text{and} \quad \|\boldsymbol{s}\|_{[L^3(\Omega)]^2}\leq C_\infty\|\boldsymbol{s}\|_{[L^\infty(\Omega)]^2}.$$

3. Well-posedness analysis of the continuous problem. We start by stating a well-known equivalence result (see [12, Chapter II, Theorem 1.1], [20, Chapter I, section 4]), adapted to the context of our problem.

LEMMA 3.1. *If $(\boldsymbol{u},p,\boldsymbol{y})\in\boldsymbol{H}_0^1(\Omega)\times L_0^2(\Omega)\times[H^1(\Omega)]^2$ solves (2.3), then $(\boldsymbol{u},\boldsymbol{y})\in\boldsymbol{X}\times[H^1(\Omega)]^2$ satisfies $\boldsymbol{y}|_\Gamma=\boldsymbol{y}^{\mathrm{D}}$ and*

$$(3.1) \qquad \begin{aligned} a(\boldsymbol{y};\boldsymbol{u},\boldsymbol{v})+c(\boldsymbol{u};\boldsymbol{u},\boldsymbol{v})-d(\boldsymbol{y},\boldsymbol{v})&=0 \quad \text{for all } \boldsymbol{v}\in\boldsymbol{X},\\ a_{\boldsymbol{y}}(\boldsymbol{y},\boldsymbol{s})+c_{\boldsymbol{y}}(\boldsymbol{u};\boldsymbol{y},\boldsymbol{s})&=0 \quad \text{for all } \boldsymbol{s}\in[H_0^1(\Omega)]^2. \end{aligned}$$

Conversely, if $(\boldsymbol{u},\boldsymbol{y})\in\boldsymbol{X}\times[H^1(\Omega)]^2$ is a solution of the reduced problem (3.1), then there exists $p\in L_0^2(\Omega)$ such that $(\boldsymbol{u},p,\boldsymbol{y})$ is a solution of (2.3).

In order to deal with the nonhomogeneous Dirichlet data appearing in the thermal energy and concentration equation, we utilize a lifting argument adapted from [37]. We write $\boldsymbol{y}$ as $\boldsymbol{y}=\boldsymbol{y}_0+\boldsymbol{y}_1$, where $\boldsymbol{y}_0\in[H_0^1(\Omega)]^2$ and $\boldsymbol{y}_1$ is such that

$$(3.2) \qquad\qquad \boldsymbol{y}_1\in[H^1(\Omega)]^2 \text{ with } \boldsymbol{y}_1|_\Gamma=\boldsymbol{y}^{\mathrm{D}}.$$

LEMMA 3.2. *If $\boldsymbol{s}^{\mathrm{D}}\in[H^{1/2}(\Gamma)]^2$, then for any $\varepsilon>0$ and $1\leq r\leq 6$ if $d=3$ or any $r\geq 1$ if $d=2$, there exists an extension $\boldsymbol{s}_1\in[H^1(\Omega)]^2$ of $\boldsymbol{s}^{\mathrm{D}}$ with $\|\boldsymbol{s}_1\|_{[L^r(\Omega)]^2}\leq\varepsilon$.*

Proof. It follows similarly as for its scalar counterpart, proven in [33, Lemma 4.1]. □

LEMMA 3.3. *Let $(\boldsymbol{u},\boldsymbol{y})$ be a solution to (3.1). Then there exist positive constants $\tilde{C}_{\boldsymbol{u}},\tilde{C}_{\boldsymbol{y}}$ such that $\|\boldsymbol{u}\|_{1,\Omega}\leq\tilde{C}_{\boldsymbol{u}}\|\boldsymbol{y}_1\|_{1,\Omega}$ and $\|\boldsymbol{y}_0\|_{1,\Omega}\leq\tilde{C}_{\boldsymbol{y}}\|\boldsymbol{y}_1\|_{1,\Omega}$.*

Proof. If one takes $\boldsymbol{v}=\boldsymbol{u}$ and $\boldsymbol{s}=\boldsymbol{y}_0$ in (3.1), then we can assert that

$$\begin{aligned} a(\boldsymbol{y}_0+\boldsymbol{y}_1;\boldsymbol{u},\boldsymbol{u})+c(\boldsymbol{u};\boldsymbol{u},\boldsymbol{u})-d(\boldsymbol{y},\boldsymbol{u})&=0,\\ a_{\boldsymbol{y}}(\boldsymbol{y}_0+\boldsymbol{y}_1,\boldsymbol{y}_0)+c_{\boldsymbol{y}}(\boldsymbol{u};\boldsymbol{y}_0+\boldsymbol{y}_1,\boldsymbol{y}_0)&=0. \end{aligned}$$

Using Remark 1, conditions (2.2), (2.4d), and Hölder's inequality, yields the estimate

(3.3) $$\alpha_a \|\boldsymbol{u}\|_{1,\Omega}^2 \le C_{\boldsymbol{F}} \big(\|\boldsymbol{y}_0\|_{1,\Omega} + \|\boldsymbol{y}_1\|_{1,\Omega} \big) \|\boldsymbol{u}\|_{1,\Omega}.$$

Similarly as above, from (2.7b), (2.8), (2.4b), and (2.6) we can derive the relation

(3.4) $$\hat{\alpha}_a \|\boldsymbol{y}_0\|_{1,\Omega}^2 \le \hat{C}_a \|\boldsymbol{y}_1\|_{1,\Omega} \|\boldsymbol{y}_0\|_{1,\Omega} + \bar{C}_v \|\boldsymbol{u}\|_{1,\Omega} \|\boldsymbol{y}_1\|_{[L^3(\Omega)]^2} \|\boldsymbol{y}_0\|_{1,\Omega}.$$

Then, substituting (3.4) back into (3.3), we obtain

$$\|\boldsymbol{u}\|_{1,\Omega} \le \frac{C_{\boldsymbol{F}}}{\alpha_a} \bigg(\frac{\hat{C}_a + \hat{\alpha}_a}{\hat{\alpha}_a} \|\boldsymbol{y}_1\|_{1,\Omega} + \frac{\bar{C}_v}{\hat{\alpha}_a} \|\boldsymbol{u}\|_{1,\Omega} \|\boldsymbol{y}_1\|_{[L^3(\Omega)]^2} \bigg),$$

which in turn implies that

$$\|\boldsymbol{u}\|_{1,\Omega} \bigg(1 - \frac{\bar{C}_v}{\hat{\alpha}_a} \|\boldsymbol{y}_1\|_{[L^3(\Omega)]^2} \bigg) \le \frac{C_{\boldsymbol{F}}(\hat{C}_a + \hat{\alpha}_a)}{\alpha_a \hat{\alpha}_a} (\|\boldsymbol{y}_1\|_{1,\Omega}).$$

In view of Lemma 3.2, we may assume that $\frac{\bar{C}_v}{\hat{\alpha}_a} \|\boldsymbol{y}_1\|_{[L^3(\Omega)]^2} \le 1/2$. Then we have

(3.5) $$\|\boldsymbol{u}\|_{1,\Omega} \le \frac{2 C_{\boldsymbol{F}}(\hat{C}_a + \hat{\alpha}_a)}{\alpha_a \hat{\alpha}_a} \|\boldsymbol{y}_1\|_{1,\Omega}.$$

Inserting (3.5) into (3.4), we are then left with

$$\begin{aligned} |\boldsymbol{y}_0|_{1,\Omega} &\le \frac{C_a}{\hat{\alpha}_a} \|\boldsymbol{y}_1\|_{1,\Omega} + \frac{2 \bar{C}_v C_{\boldsymbol{F}}(\hat{C}_a + \hat{\alpha}_a)}{\alpha_a \hat{\alpha}_a} \|\boldsymbol{y}_1\|_{[L^3(\Omega)]^2} \|\boldsymbol{y}_1\|_{1,\Omega} \\ &\le \bigg(\frac{C_a}{\hat{\alpha}_a} + \frac{C_{\boldsymbol{F}}(\hat{C}_a + \hat{\alpha}_a)}{\alpha_a} \bigg) \|\boldsymbol{y}_1\|_{1,\Omega}. \qquad \square \end{aligned}$$

THEOREM 3.1. *Assume that the conditions of section* 2.2 *hold. Then there is a lifting* $\boldsymbol{y}_1 \in [H^1(\Omega)]^2$ *of* $\boldsymbol{y}^{\mathrm{D}} \in [H^{1/2}(\Gamma)]^2$ *satisfying* (3.2) *and such that problem* (3.1) *has a solution* $(\boldsymbol{u}, \boldsymbol{y} = \boldsymbol{y}_0 + \boldsymbol{y}_1) \in \boldsymbol{H}_0^1(\Omega) \times [H^1(\Omega)]^2$. *Furthermore, there exist constants* $C_{\boldsymbol{u}}, C_{\boldsymbol{y}} > 0$ *only depending on the stability constants of section* 2.3 *such that* $\|\boldsymbol{u}\|_{1,\Omega} \le C_{\boldsymbol{u}} \|\boldsymbol{y}_1\|_{1,\Omega}$ *and* $\|\boldsymbol{y}_0\|_{1,\Omega} \le C_{\boldsymbol{y}} \|\boldsymbol{y}_1\|_{1,\Omega}$.

Proof. The result follows as an adequate modification of the proof in [33, section 4], after applying Lemma 3.3 and Brouwer's fixed-point theorem. $\square$

The assumption of additional regularity (justified for velocity in, e.g., [43, section 1.3], and for temperature and concentration in, e.g., [17, 29, 34]), along with a smallness condition allows us to establish uniqueness of solution, stated as follows.

THEOREM 3.2. *Let* $(\boldsymbol{u}, \boldsymbol{y}) \in \big[\boldsymbol{X} \cap \boldsymbol{W}^{1,\infty}(\Omega) \big] \times [H^1(\Omega) \cap L^\infty(\Omega)]^2$ *be a solution of the reduced problem* (3.1), *and assume that*

(3.6) $$\max\big\{ \|\boldsymbol{u}\|_{\boldsymbol{W}^{1,\infty}(\Omega)}, \|\boldsymbol{y}\|_{[L^\infty(\Omega)]^2}, \gamma_{\boldsymbol{F}} \big\} \le M$$

for a sufficiently small constant $M > 0$. *Then such solution is unique.*

Proof. Let $(\boldsymbol{u}, \boldsymbol{y})$, $(\tilde{\boldsymbol{u}}, \tilde{\boldsymbol{y}})$ be two solutions of problem (3.1), both satisfying assumption (3.6). Subtracting the corresponding variational formulations, we have

(3.7a) $$a(\boldsymbol{y}, \boldsymbol{u}, \boldsymbol{v}) - a(\tilde{\boldsymbol{y}}, \tilde{\boldsymbol{u}}, \boldsymbol{v}) + c(\boldsymbol{u}, \boldsymbol{u}, \boldsymbol{v}) - c(\tilde{\boldsymbol{u}}, \tilde{\boldsymbol{u}}, \boldsymbol{v}) - \big(d(\boldsymbol{y}, \boldsymbol{v}) - d(\tilde{\boldsymbol{y}}, \boldsymbol{v}) \big) = 0,$$

(3.7b) $$a_{\boldsymbol{y}}(\boldsymbol{y}, \boldsymbol{s}) - a_{\boldsymbol{y}}(\tilde{\boldsymbol{y}}, \boldsymbol{s}) + c_{\boldsymbol{y}}(\boldsymbol{u}; \boldsymbol{y}, \boldsymbol{s}) - c_{\boldsymbol{y}}(\tilde{\boldsymbol{u}}; \tilde{\boldsymbol{y}}, \boldsymbol{s}) = 0$$

for all $\boldsymbol{v} \in \boldsymbol{X}$, $\boldsymbol{s} \in [H_0^1(\Omega)]^2$. One next notices that in (3.7) one can write

$$a(\boldsymbol{y}, \boldsymbol{u}, \boldsymbol{v}) - a(\tilde{\boldsymbol{y}}, \tilde{\boldsymbol{u}}, \boldsymbol{v}) = a(\boldsymbol{y}, \boldsymbol{u} - \tilde{\boldsymbol{u}}, \boldsymbol{v}) + a(\boldsymbol{y}, \tilde{\boldsymbol{u}}, \boldsymbol{v}) - a(\tilde{\boldsymbol{y}}, \tilde{\boldsymbol{u}}, \boldsymbol{v}),$$
$$c(\boldsymbol{u}, \boldsymbol{u}, \boldsymbol{v}) - c(\tilde{\boldsymbol{u}}, \tilde{\boldsymbol{u}}, \boldsymbol{v}) = c(\boldsymbol{u}, \boldsymbol{u} - \tilde{\boldsymbol{u}}, \boldsymbol{v}) + c(\boldsymbol{u}, \tilde{\boldsymbol{u}}, \boldsymbol{v}) - c(\tilde{\boldsymbol{u}}, \tilde{\boldsymbol{u}}, \boldsymbol{v}),$$
$$c_{\boldsymbol{y}}(\boldsymbol{u}; \boldsymbol{y}, \boldsymbol{s}) - c_{\boldsymbol{y}}(\tilde{\boldsymbol{u}}; \tilde{\boldsymbol{y}}, \boldsymbol{s}) = c_{\boldsymbol{y}}(\boldsymbol{u}; \boldsymbol{y} - \tilde{\boldsymbol{y}}, \boldsymbol{s}) + c_{\boldsymbol{y}}(\boldsymbol{u}; \tilde{\boldsymbol{y}}, \boldsymbol{s}) - c_{\boldsymbol{y}}(\tilde{\boldsymbol{u}}; \tilde{\boldsymbol{y}}, \boldsymbol{s}),$$

and then we can choose as test function $\boldsymbol{v} = \boldsymbol{u} - \tilde{\boldsymbol{u}} \in \boldsymbol{X}$, and exploit (2.8) to obtain

$$a(\boldsymbol{y}, \boldsymbol{u} - \tilde{\boldsymbol{u}}, \boldsymbol{u} - \tilde{\boldsymbol{u}}) + \big(a(\boldsymbol{y}, \tilde{\boldsymbol{u}}, \boldsymbol{u} - \tilde{\boldsymbol{u}}) - a(\tilde{\boldsymbol{y}}, \tilde{\boldsymbol{u}}, \boldsymbol{u} - \tilde{\boldsymbol{u}})\big)$$
$$+ \big(c(\boldsymbol{u}; \tilde{\boldsymbol{u}}, \boldsymbol{u} - \tilde{\boldsymbol{u}}) - c(\tilde{\boldsymbol{u}}; \tilde{\boldsymbol{u}}, \boldsymbol{u} - \tilde{\boldsymbol{u}})\big) - \big(d(\boldsymbol{y}, \boldsymbol{u} - \tilde{\boldsymbol{u}}) - d(\tilde{\boldsymbol{y}}, \boldsymbol{u} - \tilde{\boldsymbol{u}})\big) = 0.$$

Applying the coercivity of the bilinear form $a(\cdot, \cdot)$ in (2.7), we readily get

(3.8)
$$\alpha_a \|\boldsymbol{u} - \tilde{\boldsymbol{u}}\|_{1,\Omega}^2 \leq \big|a(\boldsymbol{y}, \tilde{\boldsymbol{u}}, \boldsymbol{u} - \tilde{\boldsymbol{u}}) - a(\tilde{\boldsymbol{y}}, \tilde{\boldsymbol{u}}, \boldsymbol{u} - \tilde{\boldsymbol{u}})\big|$$
$$+ \big|c(\boldsymbol{u}; \tilde{\boldsymbol{u}}, \boldsymbol{u} - \tilde{\boldsymbol{u}}) - c(\tilde{\boldsymbol{u}}; \tilde{\boldsymbol{u}}, \boldsymbol{u} - \tilde{\boldsymbol{u}})\big|$$
$$+ \big|d(\boldsymbol{y}, \boldsymbol{u} - \tilde{\boldsymbol{u}}) - d(\tilde{\boldsymbol{y}}, \boldsymbol{u} - \tilde{\boldsymbol{u}})\big|.$$

Analogously, we can take $\boldsymbol{s} = \boldsymbol{y} - \tilde{\boldsymbol{y}} \in [H_0^1(\Omega)]^2$ in (3.7b), and employ the coercivity of the form $a_{\boldsymbol{y}}(\cdot, \cdot, \cdot)$ in (2.7), to eventually obtain

$$\hat{\alpha}_a \|\boldsymbol{y} - \tilde{\boldsymbol{y}}\|_{1,\Omega}^2 \leq \big|c_{\boldsymbol{y}}(\boldsymbol{u} - \tilde{\boldsymbol{u}}; \tilde{\boldsymbol{y}}, \boldsymbol{y} - \tilde{\boldsymbol{y}})\big|.$$

On the other hand, from relation (2.5) and assumption (3.6) it follows that

(3.9) $\qquad |a(\boldsymbol{y}, \tilde{\boldsymbol{u}}, \boldsymbol{u} - \tilde{\boldsymbol{u}}) - a(\tilde{\boldsymbol{y}}, \tilde{\boldsymbol{u}}, \boldsymbol{u} - \tilde{\boldsymbol{u}})| \leq \gamma_\nu M \|\boldsymbol{y} - \tilde{\boldsymbol{y}}\|_{1,\Omega} \|\boldsymbol{u} - \tilde{\boldsymbol{u}}\|_{1,\Omega}$

and, hence, replacing (3.9) in (3.8) and taking into account the continuity of the forms $c(\cdot; \cdot, \cdot)$ (stated in (2.6)) and the Lipschitz condition (2.2), we arrive at the bound

$$\alpha_a \|\boldsymbol{u} - \tilde{\boldsymbol{u}}\|_{1,\Omega}^2 \leq \gamma_\nu M \|\boldsymbol{y} - \tilde{\boldsymbol{y}}\|_{1,\Omega} \|\boldsymbol{u} - \tilde{\boldsymbol{u}}\|_{1,\Omega} + C_v \|\tilde{\boldsymbol{u}}\|_{1,\Omega} \|\boldsymbol{u} - \tilde{\boldsymbol{u}}\|_{1,\Omega}^2$$
$$+ \gamma_{\boldsymbol{F}} \|\boldsymbol{u} - \tilde{\boldsymbol{u}}\|_{1,\Omega} \|\boldsymbol{y} - \tilde{\boldsymbol{y}}\|_{1,\Omega}.$$

Proceeding in a similar manner, we can also derive the estimate

$$\hat{\alpha}_a \|\boldsymbol{y} - \tilde{\boldsymbol{y}}\|_{1,\Omega}^2 \leq \hat{C}_v \|\boldsymbol{u} - \tilde{\boldsymbol{u}}\|_{1,\Omega} \|\tilde{\boldsymbol{y}}\|_{[L^3(\Omega)]^2} \|\boldsymbol{y} - \tilde{\boldsymbol{y}}\|_{1,\Omega}.$$

Now employing (2.9) in combination with Young's inequality, we have

$$\alpha_a \|\boldsymbol{u} - \tilde{\boldsymbol{u}}\|_{1,\Omega}^2 \leq M\left(\frac{\gamma_\nu}{2} + C_v C_\infty + \frac{1}{2}\right) \|\boldsymbol{u} - \tilde{\boldsymbol{u}}\|_{1,\Omega}^2 + \frac{M}{2}(\gamma_\nu + 1) \|\boldsymbol{y} - \tilde{\boldsymbol{y}}\|_{1,\Omega}^2,$$

$$\hat{\alpha}_a \|\boldsymbol{y} - \tilde{\boldsymbol{y}}\|_{1,\Omega}^2 \leq \frac{1}{2}\bar{C}_v C_\infty M \left(\|\boldsymbol{u} - \tilde{\boldsymbol{u}}\|_{1,\Omega}^2 + \|\boldsymbol{y} - \tilde{\boldsymbol{y}}\|_{1,\Omega}^2\right).$$

Adding these inequalities and defining $\tilde{C} := (1 + \gamma_\nu + \bar{C}_v C_\infty)/2$, we get

$$\big(\alpha_a - M(C_v C_\infty + \tilde{C})\big) \|\boldsymbol{u} - \tilde{\boldsymbol{u}}\|_{1,\Omega}^2 + (\hat{\alpha}_a - M\tilde{C}) \|\boldsymbol{y} - \tilde{\boldsymbol{y}}\|_{1,\Omega}^2 \leq 0,$$

and thus uniqueness holds as long as $M < \min\{\alpha_a/(C_v C_\infty + \tilde{C}), \hat{\alpha}_a/\tilde{C}\}$. $\qquad \square$

4. Finite element discretization.

4.1. Formulation of the $\boldsymbol{H}$(div)-conforming method. Let us consider a family of regular partitions, denoted $\mathcal{T}_h$, of Ω into simplices K (triangles in two dimensions (2D) or tetrahedra in three dimensions (3D)) of diameter h_K. The mesh size will be denoted by h and, for any interior facet e in $\mathcal{E}_h$ (the set of faces in $\mathcal{T}_h$), we will label K^- and K^+ the elements adjacent to it, while h_e will stand for the length of the edge in 2D (or maximum diameter of the facet in 3D). Supposing that $\boldsymbol{v}, w$ are, respectively, smooth vector and scalar fields defined over $\mathcal{T}_h$. Then, by $(\boldsymbol{v}^\pm, w^\pm)$ we will denote the traces of $(\boldsymbol{v}, w)$ on e being the extensions from the interiors of the

elements K^+ and K^-, respectively. Let $\boldsymbol{n}_e^{\pm}$ denote the outward unit normal vector to e on $K^{\pm}$ (hence, $\boldsymbol{n}^+ = -\boldsymbol{n}^-$). We define the average $\{\!\{\cdot\}\!\}$ and jump $[\![\cdot]\!]$ operators as $\{\!\{\boldsymbol{v}\}\!\} := (\boldsymbol{v}^- + \boldsymbol{v}^+)/2$, $\{\!\{w\}\!\} := (w^- + w^+)/2$, $[\![\boldsymbol{v}]\!] := (\boldsymbol{v}^- \cdot \boldsymbol{n}_e^- + \boldsymbol{v}^+ \cdot \boldsymbol{n}_e^+)$, and $[\![w]\!] := (w^- \boldsymbol{n}_e^- + w^+ \boldsymbol{n}_e^+)$, whereas for boundary jumps and averages we adopt the convention that $\{\!\{\boldsymbol{v}\}\!\} = \boldsymbol{v}$, $[\![\boldsymbol{v}]\!] = \boldsymbol{v} \cdot \boldsymbol{n}_{\partial\Omega}$ and $\{\!\{w\}\!\} = w$, $[\![w]\!] = w\boldsymbol{n}_{\partial\Omega}$. In addition, we denote by ∇_h the broken gradient operator.

For $k \in \mathbb{N}_0$ and a mesh $\mathcal{T}_h$ on Ω, let us consider the discrete spaces (see, e.g., [11])

$$\boldsymbol{V}_h := \big\{ \boldsymbol{v}_h \in \boldsymbol{H}_0(\mathrm{div};\Omega) : \boldsymbol{v}_h|_K \in [\mathbb{P}_k(K)]^d \quad \forall K \in \mathcal{T}_h \big\},$$
$$\mathcal{Q}_h := \big\{ q_h \in L_0^2(\Omega) : q_h|_K \in \mathbb{P}_{k-1}(K) \quad \forall K \in \mathcal{T}_h \big\},$$
$$\mathcal{M}_h := \big\{ \boldsymbol{s}_h \in [C(\bar{\Omega})]^2 : \boldsymbol{s}_h|_K \in [\mathbb{P}_k(K)]^2 \quad \forall K \in \mathcal{T}_h \big\}, \qquad \mathcal{M}_{h,0} := \mathcal{M}_h \cap [H_0^1(\Omega)]^2,$$

which, in particular, satisfy $\mathrm{div}\, \boldsymbol{V}_h \subset \mathcal{Q}_h$ (cf. [28]). Here $\mathbb{P}_k(K)$ denotes the local space spanned by polynomials of degree up to k and $\boldsymbol{V}_h$ is the space of divergence-conforming BDM elements. Associated with these finite-dimensional spaces, we state the following Galerkin formulation for problem (1.1):

(4.1)

Find $(\boldsymbol{u}_h, p_h, \boldsymbol{y}_h) \in \boldsymbol{V}_h \times \mathcal{Q}_h \times \mathcal{M}_h$ such that $\boldsymbol{y}_h|_\Gamma = \boldsymbol{y}_h^{\mathrm{D}}$

and for all $(\boldsymbol{v}_h, q_h, \boldsymbol{s}_h) \in \boldsymbol{V}_h \times \mathcal{Q}_h \times \mathcal{M}_{h,0}$,

$$a^h(\boldsymbol{y}_h; \boldsymbol{u}_h, \boldsymbol{v}_h) + c^h(\boldsymbol{u}_h; \boldsymbol{u}_h, \boldsymbol{v}_h) + b(\boldsymbol{v}_h, p_h) = d(\boldsymbol{y}_h, \boldsymbol{v}_h),$$
$$b(\boldsymbol{u}_h, q_h) = 0, \quad a_{\boldsymbol{y}}(\boldsymbol{y}_h, \boldsymbol{s}_h) + c_{\boldsymbol{y}}(\boldsymbol{u}_h; \boldsymbol{y}_h, \boldsymbol{s}_h) = 0.$$

Here $\boldsymbol{y}_h^{\mathrm{D}} := \mathcal{I}_\Gamma \boldsymbol{y}^{\mathrm{D}}$ and $\mathcal{I}_\Gamma$ is the nodal interpolation operator defined in section 4.4, the discrete versions of the trilinear forms $a(\cdot; \cdot, \cdot)$ and $c(\cdot; \cdot, \cdot)$ are defined using a symmetric interior penalty and an upwind approach, respectively (see, e.g., [9, 13, 28]):

$$a^h(\boldsymbol{s}_h; \boldsymbol{u}_h, \boldsymbol{v}_h)$$
$$:= \int_\Omega \big(\boldsymbol{K}^{-1}\boldsymbol{u}_h \cdot \boldsymbol{v}_h + \nu(\boldsymbol{s}_h)\nabla_h \boldsymbol{u}_h : \nabla_h \boldsymbol{v}_h \big)$$
$$- \sum_{e \in \mathcal{E}_h} \int_e \bigg(\{\!\{\nu(\boldsymbol{s}_h)\nabla_h \boldsymbol{u}_h\}\!\} : [\![\boldsymbol{v}_h]\!] - \{\!\{\nu(\boldsymbol{s}_h)\nabla_h \boldsymbol{v}_h\}\!\} : [\![\boldsymbol{u}_h]\!] + \frac{a_0}{h_e}\nu(\boldsymbol{s}_h)[\![\boldsymbol{u}_h]\!] : [\![\boldsymbol{v}_h]\!] \bigg),$$
$$c^h(\boldsymbol{w}_h; \boldsymbol{u}_h, \boldsymbol{v}_h) := \int_\Omega (\boldsymbol{w}_h \cdot \nabla \boldsymbol{u}_h) \cdot \boldsymbol{v}_h + \sum_{K \in \mathcal{T}_h} \int_{\partial K \backslash \Gamma} \hat{\boldsymbol{w}}_h^{\mathrm{up}}(\boldsymbol{u}_h) \cdot \boldsymbol{v}_h,$$

where the fluxes are defined as $\hat{\boldsymbol{w}}_h^{\mathrm{up}}(\boldsymbol{u}_h) := \frac{1}{2}(\boldsymbol{w}_h \cdot \boldsymbol{n}_K - |\boldsymbol{w}_h \cdot \boldsymbol{n}_K|)(\boldsymbol{u}_h^e - \boldsymbol{u}_h)$, and $\boldsymbol{u}_h^e$ is the trace of $\boldsymbol{u}$ taken from within the exterior of K. As in the continuous case, we define the discrete kernel of the bilinear form $b(\cdot, \cdot)$ as

$$\boldsymbol{X}_h := \big\{ \boldsymbol{v}_h \in \boldsymbol{V}_h : b(\boldsymbol{v}_h, q_h) = 0 \ \forall q_h \in \mathcal{Q}_h \big\} = \big\{ \boldsymbol{v}_h \in \boldsymbol{V}_h : \mathrm{div}\, \boldsymbol{v}_h = 0 \text{ in } \Omega \big\}.$$

4.2. Discrete stability properties. For the sake of the subsequent analysis, we introduce the following parameter and mesh dependent broken norms:

$$\|\boldsymbol{v}\|_{*,\mathcal{T}_h}^2 := \sum_{K \in \mathcal{T}_h} \|\nabla \boldsymbol{v}\|_{0,K}^2 + \sum_{e \in \mathcal{E}_h} \frac{1}{h_e} \|[\![\boldsymbol{v}]\!]\|_{0,e}^2,$$
$$\|\boldsymbol{v}\|_{1,\mathcal{T}_h}^2 := \sigma\|\boldsymbol{v}\|_{0,\Omega}^2 + \nu_2\|\boldsymbol{v}\|_{*,\mathcal{T}_h}^2 \quad \text{for all } \boldsymbol{v} \in \boldsymbol{H}^1(\mathcal{T}_h),$$
$$\|\boldsymbol{v}\|_{2,\mathcal{T}_h}^2 := \|\boldsymbol{v}\|_{1,\mathcal{T}_h}^2 + \sum_{K \in \mathcal{T}_h} h_K^2 |\boldsymbol{v}|_{2,K}^2 \quad \text{for all } \boldsymbol{v} \in \boldsymbol{H}^2(\mathcal{T}_h),$$

where $\sigma = \|\boldsymbol{K}^{-1}\|_{\infty,\Omega}$ and ν_2 is defined in (2.1). We also recall the broken version of the well-known Sobolev embedding result (see, e.g., [21, Lemma 6.2], [27, Proposition 4.5], or [19, Theorem 5.3]): For any $r > 1$ if $d = 2$ or $1 \le r \le 6$, if $d = 3$ there exists a constant $C_{\mathrm{emb}} > 0$ such that

$$(4.2) \qquad \|\boldsymbol{v}\|_{\boldsymbol{L}^r(\Omega)} \le C_{\mathrm{emb}} \|\boldsymbol{v}\|_{1,\mathcal{T}_h} \qquad \text{for all } \boldsymbol{v} \in \boldsymbol{H}^1(\mathcal{T}_h).$$

Moreover, we will use the broken space

$$\boldsymbol{C}^1(\mathcal{T}_h) := \left\{ \boldsymbol{u} \in \boldsymbol{H}^1(\mathcal{T}_h) : \boldsymbol{u}|_K \in \boldsymbol{C}^1(\bar{K}), K \in \mathcal{T}_h \right\},$$

equipped with an appropriate norm $\|\boldsymbol{u}\|_{\boldsymbol{W}^{1,\infty}(\mathcal{T}_h)} := \max_{K \in \mathcal{T}_h} \|\boldsymbol{u}\|_{\boldsymbol{W}^{1,\infty}(K)}$. Finally, we will also use an augmented H^1-norm defined as

$$\|\boldsymbol{s}\|_{1,\mathcal{E}_h} := \|\boldsymbol{s}\|_{1,\Omega}^2 + \sum_{e \in \mathcal{E}_h} \frac{1}{h_e} \|\boldsymbol{s}\|_{0,e}^2 \qquad \text{for all } \boldsymbol{s} \in [H^1(\Omega)]^2.$$

Using these norms, and the local trace inequalities

$$\|\boldsymbol{v}\|_{0,\partial K} \le C(h_K^{-1/2} \|\boldsymbol{v}\|_{0,K} + h_K^{1/2} |\boldsymbol{v}|_{1,K}) \quad \text{for all } \boldsymbol{v} \in \boldsymbol{H}^1(K),$$
$$\|p\|_{0,\partial K} \le C h_K^{-1/2} \|p\|_{0,K} \quad \text{for all } p \in \mathbb{P}_k(K),$$

we can establish continuity of the trilinear and bilinear forms involved, stated in the following lemma that can be proved following [37, section 3.3.2] and [9, section 4].

LEMMA 4.1. *The following properties hold:*

$$(4.3\text{a}) \qquad \left| a^h(\cdot, \boldsymbol{u}, \boldsymbol{v}) \right| \le C \|\boldsymbol{u}\|_{2,\mathcal{T}_h} \|\boldsymbol{v}\|_{1,\mathcal{T}_h} \qquad \text{for all } \boldsymbol{u} \in \boldsymbol{H}^2(\mathcal{T}_h), \boldsymbol{v} \in \boldsymbol{V}_h,$$

$$(4.3\text{b}) \qquad \left| a^h(\cdot, \boldsymbol{u}, \boldsymbol{v}) \right| \le \tilde{C}_a \|\boldsymbol{u}\|_{1,\mathcal{T}_h} \|\boldsymbol{v}\|_{1,\mathcal{T}_h} \qquad \text{for all } \boldsymbol{u}, \boldsymbol{v} \in \boldsymbol{V}_h,$$

$$(4.3\text{c}) \qquad \left| b(\boldsymbol{v}, q) \right| \le \|\boldsymbol{v}\|_{1,\mathcal{T}_h} \|q\|_{0,\Omega} \qquad \text{for all } \boldsymbol{v} \in \boldsymbol{H}^1(\mathcal{T}_h), q \in L_0^2(\Omega),$$

and for all $\boldsymbol{u}, \boldsymbol{v}, \boldsymbol{w} \in \boldsymbol{H}^1(\mathcal{T}_h)$ and $\boldsymbol{s}, \boldsymbol{y} \in [H^1(\Omega)]^2$,

$$(4.4\text{a}) \qquad \left| d(\boldsymbol{y}, \boldsymbol{v}) \right| \le C_{\boldsymbol{F}} \|\boldsymbol{y}\|_{1,\Omega} \|\boldsymbol{v}\|_{1,\mathcal{T}_h},$$

$$(4.4\text{b}) \qquad \left| c_{\boldsymbol{y}}(\boldsymbol{w}; \boldsymbol{y}, \boldsymbol{s}) \right| \le \tilde{C}_1 \|\boldsymbol{w}\|_{1,\mathcal{T}_h} \|\boldsymbol{s}\|_{1,\Omega} \|\boldsymbol{y}\|_{1,\Omega},$$

$$(4.4\text{c}) \qquad \left| c_{\boldsymbol{y}}(\boldsymbol{w}; \boldsymbol{y}, \boldsymbol{s}) \right| \le \tilde{C}_2 \|\boldsymbol{w}\|_{1,\mathcal{T}_h} \|\boldsymbol{y}\|_{[L^3(\Omega)]^2} \|\nabla \boldsymbol{s}\|_{0,\Omega}.$$

Moreover, for $\boldsymbol{s}_1, \boldsymbol{s}_2 \in [H^1(\Omega)]^2$, $\boldsymbol{u} \in \boldsymbol{C}^1(\mathcal{T}_h)$, and $\boldsymbol{v} \in \boldsymbol{V}_h$, there holds

$$(4.5) \qquad \left| a^h(\boldsymbol{s}_1; \boldsymbol{u}, \boldsymbol{v}) - a^h(\boldsymbol{s}_2; \boldsymbol{u}, \boldsymbol{v}) \right| \le \tilde{C}_{\mathrm{Lip}} \gamma_\nu \|\boldsymbol{s}_1 - \boldsymbol{s}_2\|_{1,\mathcal{E}_h} \|\boldsymbol{u}\|_{\boldsymbol{W}^{1,\infty}(\mathcal{T}_h)} \|\boldsymbol{v}\|_{1,\mathcal{T}_h},$$

where the constant $\tilde{C}_{\mathrm{Lip}} > 0$ is independent of h (cf. [37, Lemma 3.3]). A related result follows for $c^h(\cdot; \cdot, \cdot)$ as in [37, Lemma 3.4]. Let $\boldsymbol{w}_1, \boldsymbol{w}_2, \boldsymbol{u} \in \boldsymbol{H}^2(\mathcal{T}_h)$ and $\boldsymbol{v} \in V_h$. Then there exists $\tilde{C}_v > 0$ independently of h such that

$$(4.6) \qquad \left| c^h(\boldsymbol{w}_1; \boldsymbol{u}, \boldsymbol{v}) - c^h(\boldsymbol{w}_2; \boldsymbol{u}, \boldsymbol{v}) \right| \le \tilde{C}_v \|\boldsymbol{w}_1 - \boldsymbol{w}_2\|_{1,\mathcal{T}_h} \|\boldsymbol{u}\|_{1,\mathcal{T}_h} \|\boldsymbol{v}\|_{1,\mathcal{T}_h}.$$

While the coercivity of the form $a_{\boldsymbol{y}}(\cdot, \cdot)$ in the discrete setting is readily implied by (2.7), there also holds (cf. [28, Lemma 3.2])

$$(4.7) \qquad a^h(\cdot, \boldsymbol{v}, \boldsymbol{v}) \ge \tilde{\alpha}_a \|\boldsymbol{v}\|_{1,\mathcal{T}_h}^2 \quad \text{for all } \boldsymbol{v} \in \boldsymbol{V}_h,$$

provided that $a_0 > 0$ is sufficiently large and independent of the mesh size.

Let $\boldsymbol{w} \in \boldsymbol{H}_0(\mathrm{div}^0; \Omega)$, then, according to [37] we can write

$$(4.8) \qquad c^h(\boldsymbol{w}; \boldsymbol{u}, \boldsymbol{u}) = \frac{1}{2} \sum_{e \in \mathcal{E}_h^i} \int_e |\boldsymbol{w} \cdot \boldsymbol{n}_e| |[\![\boldsymbol{v}]\!]|^2 \geq 0 \quad \text{for all } \boldsymbol{u} \in \boldsymbol{V}_h,$$

as well as the following relation

$$(4.9) \qquad c_{\boldsymbol{y}}(\boldsymbol{w}; \boldsymbol{s}_h, \boldsymbol{s}_h) = 0 \quad \text{for all } \boldsymbol{s}_h \in \mathcal{M}_h,$$

which arises from integration by parts and holds at the discrete level since the produced discrete velocities are exactly divergence free. Finally, we recall from [28] the following discrete inf-sup condition for $b(\cdot, \cdot)$, where $\tilde{\beta}$ is independent of h:

$$(4.10) \qquad \sup_{\boldsymbol{v}_h \in \boldsymbol{V}_h \backslash \{\boldsymbol{0}\}} \frac{b(\boldsymbol{v}_h, q_h)}{\|\boldsymbol{v}_h\|_{1, \mathcal{T}_h}} \geq \tilde{\beta} \|q_h\|_{0, \Omega} \quad \text{for all } q_h \in \mathcal{Q}_h.$$

4.3. Existence of discrete solutions. Due to the discrete stability properties stated in the previous section, a discrete analogue of Lemma 3.1 holds.

LEMMA 4.2. *If $(\boldsymbol{u}_h, p_h, \boldsymbol{y}_h) \in \boldsymbol{V}_h \times \mathcal{Q}_h \times \mathcal{M}_h$ is a solution of (4.1), then $\boldsymbol{u}_h \in \boldsymbol{X}_h$, and $(\boldsymbol{u}_h, \boldsymbol{y}_h)$ is a solution of the discrete reduced problem*

$$(4.11) \qquad \begin{aligned} a^h(\boldsymbol{y}_h; \boldsymbol{u}_h, \boldsymbol{v}) + c^h(\boldsymbol{u}_h; \boldsymbol{u}_h, \boldsymbol{v}) - d(\boldsymbol{y}_h, \boldsymbol{v}) &= 0, \\ a_{\boldsymbol{y}}(\boldsymbol{y}_h, \boldsymbol{s}) + c_{\boldsymbol{y}}(\boldsymbol{u}_h; \boldsymbol{y}_h, \boldsymbol{s}) &= 0 \quad \text{for all } (\boldsymbol{v}, \boldsymbol{s}) \in \boldsymbol{X}_h \times \mathcal{M}_{h,0}. \end{aligned}$$

Conversely, if $(\boldsymbol{u}_h, \boldsymbol{y}_h) \in \boldsymbol{X}_h \times \mathcal{M}_{h,0}$ is a solution of (4.11), then there exists a unique pressure $p_h \in \mathcal{Q}_h$ such that $(\boldsymbol{u}_h, p_h, \boldsymbol{y}_h)$ is a solution to (4.1).

As in the continuous case, we also perform a boundary lifting of $\boldsymbol{y}_h$ by setting $\boldsymbol{y}_h = \boldsymbol{y}_{h,0} + \boldsymbol{y}_{h,1}$ with $\boldsymbol{y}_{h,0} \in \mathcal{M}_{h,0}$, and

$$(4.12) \qquad \boldsymbol{y}_{h,1} \in \mathcal{M}_h, \quad \boldsymbol{y}_{h,1}|_\Gamma = \boldsymbol{y}_h^{\mathrm{D}}.$$

LEMMA 4.3. *Let $(\boldsymbol{u}_h, \boldsymbol{y}_h)$ be a solution of (4.11) with $\boldsymbol{y}_h = \boldsymbol{y}_{h,0} + \boldsymbol{y}_{h,1}$ as in (4.12). Assume that*

$$(4.13) \qquad C_{\mathrm{dep}} \|\boldsymbol{y}_{h,1}\|_{[L^3(\Omega)]^2} \leq \frac{1}{2}, \quad \text{where} \quad C_{\mathrm{dep}} = \frac{\tilde{C}_{\boldsymbol{F}} \tilde{C}_2}{\tilde{\alpha}_a \hat{\alpha}_a}.$$

Then there exist constants $\tilde{C}_{\boldsymbol{u}}, \tilde{C}_{\boldsymbol{y}} > 0$ only depending on the stability constants from section 4.2, such that

$$(4.14) \qquad \|\boldsymbol{u}\|_{1, \mathcal{T}_h} \leq \tilde{C}_u \|\boldsymbol{y}_{h,1}\|_{1, \Omega} \quad \text{and} \quad \|\boldsymbol{y}_h\|_{1, \Omega} \leq \tilde{C}_{\boldsymbol{y}} \|\boldsymbol{y}_{h,1}\|_{1, \Omega}.$$

Proof. We choose $(\boldsymbol{v}, \boldsymbol{s}) = (\boldsymbol{u}_h, \boldsymbol{y}_{h,0})$ in (4.11) and use (4.8)–(4.9) to obtain

$$a^h(\boldsymbol{y}_h; \boldsymbol{u}_h, \boldsymbol{u}_h) = d(\boldsymbol{y}_h, \boldsymbol{u}_h), \quad a_{\boldsymbol{y}}(\boldsymbol{y}_{h,0}, \boldsymbol{y}_{h,0}) + a_{\boldsymbol{y}}(\boldsymbol{y}_{h,1}, \boldsymbol{y}_{h,0}) = -c_{\boldsymbol{y}}(\boldsymbol{u}_h; \boldsymbol{y}_{h,1}, \boldsymbol{y}_{h,0}).$$

Invoking the coercivity of the forms $a_h(\cdot; \cdot, \cdot)$ and $a_{\boldsymbol{y}}(\cdot, \cdot)$ in (4.7), (2.7b) and the boundedness of $c_{\boldsymbol{y}}(\cdot; \cdot, \cdot)$, $d(\cdot, \cdot)$ stated in (4.4c), (4.4a), we have

$$(4.15\mathrm{a}) \qquad \tilde{\alpha}_a \|\boldsymbol{u}_h\|_{1, \mathcal{T}_h} \leq \tilde{C}_{\boldsymbol{F}} (\|\boldsymbol{y}_{h,0}\|_{1, \Omega} + \|\boldsymbol{y}_{h,1}\|_{1, \Omega}),$$

$$(4.15\mathrm{b}) \qquad \hat{\alpha}_a \|\boldsymbol{y}_{h,0}\|_{1, \Omega} \leq \hat{C}_a \|\boldsymbol{y}_{h,1}\|_{1, \Omega} + \tilde{C}_2 \|\boldsymbol{y}_{h,1}\|_{[L^3(\Omega)]^2} \|\boldsymbol{u}\|_{1, \mathcal{T}_h}.$$

Substituting (4.15b) into (4.15a) then leads to

$$\tilde{\alpha}_a \|\boldsymbol{u}_h\|_{1,\mathcal{T}_h} \leq \tilde{C}_{\boldsymbol{F}} \left(\|\boldsymbol{y}_{h,1}\|_{1,\Omega} + \frac{\hat{C}_a}{\hat{\alpha}_a} \|\boldsymbol{y}_{h,1}\|_{1,\Omega} + \frac{\tilde{C}_2}{\hat{\alpha}_a} \|\boldsymbol{y}_{h,1}\|_{[L^3(\Omega)]^2} \|\boldsymbol{u}\|_{1,\mathcal{T}_h} \right),$$

$$\|\boldsymbol{u}_h\|_{1,\mathcal{T}_h} \leq C_{\text{dep}} \|\boldsymbol{y}_{h,1}\|_{[L^3(\Omega)]^2} + \frac{C_{\boldsymbol{F}}}{\tilde{\alpha}_a} \left(1 + \frac{\hat{C}_a}{\hat{\alpha}_a} \right) \|\boldsymbol{y}_{h,1}\|_{1,\Omega} \leq \tilde{C}_{\boldsymbol{u}} \|\boldsymbol{y}_{h,1}\|_{1,\Omega},$$

where $\tilde{C}_{\boldsymbol{u}} = 2 \frac{C_{\boldsymbol{F}}}{\tilde{\alpha}_a} (1 + \frac{\hat{C}_a}{\hat{\alpha}_a})$. Finally, the definition of the discrete liftings and an application of the triangle inequality imply that

$$\begin{aligned}
\|\boldsymbol{y}_h\|_{1,\Omega} &\leq \frac{\hat{C}_a}{\hat{\alpha}_a} \|\boldsymbol{y}_{h,1}\|_{1,\Omega} + \frac{\tilde{C}_2}{\hat{\alpha}_a} \|\boldsymbol{y}_{h,1}\|_{[L^3(\Omega)]^2} \|\boldsymbol{u}_h\|_{1,\mathcal{T}_h} + \|\boldsymbol{y}_{h,1}\|_{1,\Omega} \\
&\leq \frac{\hat{C}_a + \hat{\alpha}_a}{\hat{\alpha}_a} \|\boldsymbol{y}_{h,1}\|_{1,\Omega} + \frac{\tilde{C}_2}{\hat{\alpha}_a} \|\boldsymbol{y}_{h,1}\|_{[L^3(\Omega)]^2} 2 C_{\boldsymbol{F}} \frac{\hat{C}_a + \hat{\alpha}_a}{\tilde{\alpha}_a \hat{\alpha}_a} \|\boldsymbol{y}_{h,1}\|_{1,\Omega} \\
&\leq 2 \frac{\hat{C}_a + \hat{\alpha}_a}{\hat{\alpha}_a} \|\boldsymbol{y}_{h,1}\|_{1,\Omega} \leq \tilde{C}_{\boldsymbol{y}} \|\boldsymbol{y}_{h,1}\|_{1,\Omega}. \qquad \square
\end{aligned}$$

THEOREM 4.1. *Let $\boldsymbol{y}_{h,1}$ be a discrete lifting satisfying (4.13). Then there exists a discrete solution $(\boldsymbol{u}_h, \boldsymbol{y}_h) \in \boldsymbol{X}_h \times \mathcal{M}_h$ to (4.11) satisfying the stability bound (4.14).*

Proof. We shall make use of Brouwer's fixed-point theorem in the following form: *Let $\mathcal{K} \neq \varnothing$ be a nonempty compact convex subset of a finite-dimensional normed space, and let $\mathcal{L} : \mathcal{K} \to \mathcal{K}$ be a continuous mapping. Then $\mathcal{L}$ has at least one fixed point in $\mathcal{K}$.* Let us then start by defining the following finite-dimensional set, where $\tilde{C}_{\boldsymbol{u}}$ is the constant from (4.14):

$$\mathcal{K}_1 = \left\{ \boldsymbol{w}_h \in \boldsymbol{X}_h : \|\boldsymbol{w}_h\|_{1,\mathcal{T}_h} \leq \tilde{C}_{\boldsymbol{u}} \|\boldsymbol{y}_{h,1}\|_{1,\Omega} \right\}.$$

Note that $\mathcal{K}_1$ is convex and compact. Next we define the mapping $\boldsymbol{T} : \mathcal{K}_1 \to \mathcal{K}_1$, $\boldsymbol{w}_h \mapsto \boldsymbol{T}(\boldsymbol{w}_h) = \boldsymbol{u}_h$, where $\boldsymbol{u}_h$ is the first component of the solution of the following linearized version of problem (4.11):

(4.16)
$$\begin{aligned}
&\text{Find } (\boldsymbol{u}_h, \boldsymbol{y}_h) \in \boldsymbol{X}_h \times \mathcal{M}_h \text{ such that for all } (\boldsymbol{v}, \boldsymbol{s}) \in \boldsymbol{X}_h \times \mathcal{M}_{h,0}, \\
&a^h(\boldsymbol{y}_h; \boldsymbol{u}_h, \boldsymbol{v}) + c^h(\boldsymbol{w}_h; \boldsymbol{u}_h, \boldsymbol{v}) - d(\boldsymbol{y}_h, \boldsymbol{v}) = 0, \\
&a_{\boldsymbol{y}}(\boldsymbol{y}_{h,0}, \boldsymbol{s}) + c_{\boldsymbol{y}}(\boldsymbol{w}_h; \boldsymbol{y}_{h,0}, \boldsymbol{s}) = -a_{\boldsymbol{y}}(\boldsymbol{y}_{h,1}, \boldsymbol{s}) - c_{\boldsymbol{y}}(\boldsymbol{w}_h; \boldsymbol{y}_{h,1}, \boldsymbol{s}).
\end{aligned}$$

Clearly, we have the equivalence

$$\boldsymbol{T}(\boldsymbol{u}_h) = \boldsymbol{u}_h \iff (\boldsymbol{u}_h, \boldsymbol{y}_h) \in \boldsymbol{X}_h \times \mathcal{M}_h \text{ satisfies (4.11)}$$

and, owing to Lemma 4.2, we also get

$$\boldsymbol{T}(\boldsymbol{u}_h) = \boldsymbol{u}_h \iff (\boldsymbol{u}_h, \boldsymbol{y}_h, p_h) \in \boldsymbol{V}_h \times \mathcal{M}_h \times \mathcal{Q}_h \text{ satisfies (4.1)}.$$

In order to prove that the discrete fixed-point operator $\boldsymbol{T}$ is well-defined, we define the following sets, where $\tilde{C}_{\boldsymbol{u}}$ and $\tilde{C}_{\boldsymbol{y}}$ are the constants from (4.14):

$$\mathcal{K} := \left\{ (\boldsymbol{w}_h, \boldsymbol{\varphi}_h) \in \boldsymbol{X}_h \times \mathcal{M}_h : \|\boldsymbol{w}_h\|_{1,\mathcal{T}_h} \leq \tilde{C}_{\boldsymbol{u}} \|\boldsymbol{y}_{h,1}\|_{1,\Omega}, \|\boldsymbol{\varphi}_h\|_{1,\Omega} \leq \tilde{C}_{\boldsymbol{y}} \|\boldsymbol{y}_{h,1}\|_{1,\Omega} \right\},$$
$$\mathcal{K}_2 := \left\{ \boldsymbol{\varphi}_h \in \mathcal{M}_h : \|\boldsymbol{\varphi}_h\|_{1,\Omega} \leq \tilde{C}_{\boldsymbol{y}} \|\boldsymbol{y}_{h,1}\|_{1,\Omega} \right\},$$

and introduce the discrete operator $\boldsymbol{R} : \mathcal{K} \to \mathcal{K}_1$, $(\boldsymbol{w}_h, \boldsymbol{\varphi}_h) \mapsto \boldsymbol{R}((\boldsymbol{w}_h, \boldsymbol{\varphi}_h)) = \boldsymbol{u}_h$, where $\boldsymbol{u}_h$ is the unique solution to the problem

$$(4.17) \qquad \begin{aligned} &\text{find } \boldsymbol{u}_h \in \boldsymbol{X}_h \text{ such that for all } \boldsymbol{v} \in \boldsymbol{X}_h, \\ &a^h(\boldsymbol{\varphi}_h; \boldsymbol{u}_h, \boldsymbol{v}) + c^h(\boldsymbol{w}_h; \boldsymbol{u}_h, \boldsymbol{v}) - d(\boldsymbol{\varphi}_h, \boldsymbol{v}) = 0, \end{aligned}$$

and similarly define the discrete map $\boldsymbol{S} : \mathcal{K}_1 \to \mathcal{K}_2$, $\boldsymbol{w}_h \mapsto \boldsymbol{S}(\boldsymbol{w}_h) = \boldsymbol{y}_h$, where $\boldsymbol{y}_h \in \mathcal{M}_h$ is the unique solution of the problem

$$(4.18) \qquad \begin{aligned} &\text{find } \boldsymbol{y}_h \in \mathcal{M}_h \text{ such that for all } \boldsymbol{s} \in \mathcal{M}_{h,0}, \\ &a_{\boldsymbol{y}}(\boldsymbol{y}_{h,0}, \boldsymbol{s}) + c_{\boldsymbol{y}}(\boldsymbol{w}_h; \boldsymbol{y}_{h,0}, \boldsymbol{s}) = -a_{\boldsymbol{y}}(\boldsymbol{y}_{h,1}, \boldsymbol{s}) - c_{\boldsymbol{y}}(\boldsymbol{w}_h; \boldsymbol{y}_{h,1}). \end{aligned}$$

Clearly, $\boldsymbol{T}$ can be rewritten as $\boldsymbol{T}(\boldsymbol{w}_h) = \boldsymbol{R}(\boldsymbol{w}_h, \boldsymbol{S}(\boldsymbol{w}_h))$, so to prove its well-definiteness, it suffices to show that $\boldsymbol{R}$ and $\boldsymbol{S}$ are well-defined. We begin with operator $\boldsymbol{R}$. Since for any $\boldsymbol{w}_h \in \boldsymbol{X}_h$ and $\boldsymbol{\varphi}_h \in [H^1(\Omega)]^2$ the bilinear form $a^h(\boldsymbol{\varphi}_h; \cdot, \cdot) + c^h(\boldsymbol{w}_h, \cdot, \cdot)$ is $\boldsymbol{V}_h$-elliptic (thanks to (4.7) and (4.8)), existence and uniqueness follow from the Lax–Milgram lemma. Moreover, selecting $\boldsymbol{v} = \boldsymbol{u}_h$ in (4.17), we can appeal to the coercivity of $a^h(\cdot; \cdot, \cdot)$, the positivity of $c^h(\cdot; \cdot, \cdot)$ (4.8), condition (4.13), the bound for $d(\cdot, \cdot)$ stated in (4.4a), and the bounds within the definition of $\mathcal{K}$ to deduce that

$$\|\boldsymbol{u}_h\|_{1,\mathcal{T}_h}^2 \leq \frac{C_{\boldsymbol{F}}}{\tilde{\alpha}_a} \|\boldsymbol{\varphi}_h\|_{1,\Omega} \|\boldsymbol{u}_h\|_{1,\mathcal{T}_h},$$

$$\|\boldsymbol{u}_h\|_{1,\mathcal{T}_h} \leq \frac{C_{\boldsymbol{F}} \tilde{C}_{\boldsymbol{y}}}{\tilde{\alpha}_a} \|\boldsymbol{y}_{h,1}\|_{1,\Omega} \leq 2 C_{\boldsymbol{F}} \frac{\tilde{\alpha}_a + \hat{C}_a}{\tilde{\alpha}_a \hat{\alpha}_a} \|\boldsymbol{y}_{h,1}\|_{1,\Omega} \leq \tilde{C}_{\boldsymbol{u}} \|\boldsymbol{y}_{h,1}\|_{1,\Omega},$$

which implies that $\boldsymbol{u}_h \in \mathcal{K}_1$.

Analogously, for $\boldsymbol{S}$ we note that thanks to (2.7b) and (4.9), the bilinear form $a_{\boldsymbol{y}}(\cdot, \cdot) + c^h(\boldsymbol{w}_h, \cdot, \cdot)$ is $\mathcal{M}_{h,0}$-elliptic, hence, for a fixed discrete lifting $\boldsymbol{y}_{h,1}$, the homogeneous counterpart to the linear problem (4.18) has a unique solution. Proceeding as done above for (4.16), we use once more the coercivity of $a_{\boldsymbol{y}}(\cdot, \cdot)$ (2.4b), (4.9), condition (4.13), the bound (4.4c) for $c_{\boldsymbol{y}}(\cdot; \cdot, \cdot)$, and the definition of $\mathcal{K}_1$ to find that

$$\|\boldsymbol{y}_{h,0}\|_{1,\Omega}^2 \leq \frac{\tilde{C}_a}{\hat{\alpha}_a} \|\boldsymbol{y}_{h,1}\|_{1,\Omega} \|\boldsymbol{y}_{h,0}\|_{1,\Omega} + \frac{\tilde{C}_2}{\hat{\alpha}_a} \|\boldsymbol{y}_{h,1}\|_{[L^3(\Omega)]^2} \|\boldsymbol{w}_h\|_{1,\mathcal{T}_h} \|\boldsymbol{y}_{h,0}\|_{1,0},$$

$$\begin{aligned} \|\boldsymbol{y}_{h,0}\|_{1,\Omega} &\leq \frac{\hat{C}_a}{\hat{\alpha}_a} \|\boldsymbol{y}_{h,1}\|_{1,\Omega} + \frac{\tilde{C}_2}{\hat{\alpha}_a} \|\boldsymbol{y}_{h,1}\|_{[L^3(\Omega)]^2} 2 C_{\boldsymbol{F}} \frac{\tilde{\alpha}_a + \hat{C}_a}{\tilde{\alpha}_a \hat{\alpha}_a} \|\boldsymbol{y}_{h,1}\|_{1,\Omega} \\ &\leq 2 \frac{\hat{\alpha}_a + \hat{C}_a}{\hat{\alpha}_a} \|\boldsymbol{y}_{h,1}\|_{1,\Omega}. \end{aligned}$$

We then employ the triangle inequality to obtain

$$\|\boldsymbol{y}_h\|_{1,\Omega} \leq 2 \frac{\hat{\alpha}_a + \hat{C}_a}{\hat{\alpha}_a} \|\boldsymbol{y}_{h,1}\|_{1,\Omega} + \|\boldsymbol{y}_{h,1}\|_{1,\Omega} \leq \tilde{C}_{\boldsymbol{y}} \|\boldsymbol{y}_{h,1}\|_{1,\Omega},$$

hence establishing that $\boldsymbol{y}_h \in \mathcal{K}_2$.

In order to apply Brouwer's theorem, it remains to show that $\boldsymbol{R}$ and $\boldsymbol{S}$ are continuous operators. Let us assume we are given $(\boldsymbol{w}, \boldsymbol{\varphi}) \in \mathcal{K}$ and a sequence $\{(\boldsymbol{w}_l, \boldsymbol{\varphi}_l)\}_{l \in \mathbb{N}} \subset \mathcal{K}$ such that $\|\boldsymbol{w}_l - \boldsymbol{w}\|_{1,\mathcal{T}_h} \to 0$ and $\|\boldsymbol{\varphi}_l - \boldsymbol{\varphi}\|_{1,\Omega} \to 0$ as $l \to \infty$.

From the definition of $\boldsymbol{R}$ (cf. (4.17)) the following relations can be derived:

$$a^h(\boldsymbol{\varphi}_l; \boldsymbol{u}_l, \boldsymbol{v}) + c^h(\boldsymbol{w}_l; \boldsymbol{u}_l, \boldsymbol{v}) - d(\boldsymbol{\varphi}_l, \boldsymbol{v}) = 0,$$
$$a^h(\boldsymbol{\varphi}; \boldsymbol{u}, \boldsymbol{v}) + c^h(\boldsymbol{w}; \boldsymbol{u}, \boldsymbol{v}) - d(\boldsymbol{\varphi}, \boldsymbol{v}) = 0 \quad \text{for all } \boldsymbol{v} \in \boldsymbol{X}_h.$$

Subtracting these two systems from each other and rearranging terms yields

$$a^h(\boldsymbol{\varphi}_l; \boldsymbol{u} - \boldsymbol{u}_l, \boldsymbol{v}) + c^h(\boldsymbol{w}_l; \boldsymbol{u} - \boldsymbol{u}_l, \boldsymbol{v}) = -a^h(\boldsymbol{\varphi}; \boldsymbol{u}, \boldsymbol{v}) + a^h(\boldsymbol{\varphi}_l; \boldsymbol{u}, \boldsymbol{v}) - c^h(\boldsymbol{w}; \boldsymbol{u}, \boldsymbol{v})$$
$$+ c^h(\boldsymbol{w}_l; \boldsymbol{u}, \boldsymbol{v}) + d(\boldsymbol{\varphi}_l, \boldsymbol{v}) - d(\boldsymbol{\varphi}, \boldsymbol{v})$$

for all $\boldsymbol{v} \in \boldsymbol{X}_h$. We can take in particular $\boldsymbol{v} = \boldsymbol{u} - \boldsymbol{u}_l$, and exploit the coercivity of $a^h(\cdot; \cdot, \cdot)$, the fact that $c^h(\cdot, \boldsymbol{u} - \boldsymbol{u}_l, \boldsymbol{u} - \boldsymbol{u}_l) > 0$, the boundedness of $c^h(\cdot; \cdot, \cdot)$ (4.6) in combination with the bounds for $d(\cdot, \cdot)$, as well as property (4.5), to eventually get

$$\|\boldsymbol{u} - \boldsymbol{u}_l\|_{1,\mathcal{T}_h} \leq \frac{1}{\tilde{\alpha}_a} \big(\tilde{C}_{\text{Lip}} \gamma_\nu \|\boldsymbol{\varphi} - \boldsymbol{\varphi}_l\|_{1,\mathcal{E}_h} \|\boldsymbol{u}\|_{\boldsymbol{W}^{1,\infty}(\mathcal{T}_h)}$$
$$+ \tilde{C}_v \|\boldsymbol{w} - \boldsymbol{w}_l\|_{1,\mathcal{T}_h} \|\boldsymbol{u}\|_{1,\mathcal{T}_h} + \gamma_{\boldsymbol{F}} \|\boldsymbol{\varphi} - \boldsymbol{\varphi}_l\|_{1,\Omega} \big)$$
$$\leq C \big(\|\boldsymbol{\varphi} - \boldsymbol{\varphi}_l\|_{1,\mathcal{E}_h} \|\boldsymbol{u}\|_{\boldsymbol{W}^{1,\infty}(\mathcal{T}_h)} + \|\boldsymbol{w} - \boldsymbol{w}_l\|_{1,\mathcal{T}_h} \|\boldsymbol{u}\|_{1,\mathcal{T}_h} + \|\boldsymbol{\varphi} - \boldsymbol{\varphi}_l\|_{1,\Omega} \big)$$

and, hence, $\|\boldsymbol{u} - \boldsymbol{u}_l\|_{1,\mathcal{T}_h} \to 0$ as $l \to \infty$.

Next we consider the definition of $\boldsymbol{S}$ (4.18) and again we consider the relations

$$a_{\boldsymbol{y}}(\boldsymbol{y}_l, \boldsymbol{s}) + c_{\boldsymbol{y}}(\boldsymbol{w}_l; \boldsymbol{y}_l, \boldsymbol{s}) = 0, \quad a_{\boldsymbol{y}}(\boldsymbol{y}, \boldsymbol{s}) + c_{\boldsymbol{y}}(\boldsymbol{w}; \boldsymbol{y}, \boldsymbol{s}) = 0 \quad \text{for all } \boldsymbol{s} \in \mathcal{M}_{h,0}.$$

Subtracting the second system from the first leads to

$$a_{\boldsymbol{y}}(\boldsymbol{y}_l - \boldsymbol{y}, \boldsymbol{s}) + c_{\boldsymbol{y}}(\boldsymbol{w}_l; \boldsymbol{y} - \boldsymbol{y}_l, \boldsymbol{s}) = -c_{\boldsymbol{y}}(\boldsymbol{w}; \boldsymbol{y}, \boldsymbol{s}) - c_{\boldsymbol{y}}(\boldsymbol{w}_l; \boldsymbol{y}, \boldsymbol{s}).$$

Now we take $\boldsymbol{s} = \boldsymbol{y} - \boldsymbol{y}_l \in \mathcal{M}_{h,0}$ and immediately note that $c_{\boldsymbol{y}}(\boldsymbol{w}_l; \boldsymbol{y} - \boldsymbol{y}_l, \boldsymbol{y} - \boldsymbol{y}_l) = 0$, to (4.9). Using the coercivity of $a_{\boldsymbol{y}}(\cdot; \cdot, \cdot)$ in (2.4b) together with the boundedness of $c_{\boldsymbol{y}}(\cdot; \cdot, \cdot)$, we have

$$\|\boldsymbol{y} - \boldsymbol{y}_l\|_{1,\Omega}^2 \leq \frac{\tilde{C}_2}{\hat{\alpha}_a} \|\boldsymbol{w} - \boldsymbol{w}_l\|_{1,\mathcal{T}_h} \|\boldsymbol{y}\|_{[L^3(\Omega)]^2} \|\boldsymbol{y} - \boldsymbol{y}_l\|_{1,\Omega},$$

thus $\|\boldsymbol{y} - \boldsymbol{y}_l\|_{1,\Omega} \leq C \|\boldsymbol{w} - \boldsymbol{w}_l\|_{1,\mathcal{T}_h} \|\boldsymbol{y}\|_{[L^3(\Omega)]^2}$ and so $\|\boldsymbol{y} - \boldsymbol{y}_l\|_{1,\Omega} \to 0$ as $l \to \infty$. $\square$

Note that unlike conforming discretizations, one cannot directly establish a discrete version of Theorem 3.2. In fact we were not able to control the augmented norm $\|\cdot\|_{1,\mathcal{E}_h}$ in a way reciprocal to that used to prove that theorem. However, even when uniqueness of the discrete counterpart remains an open problem, our nonexhaustive selection of numerical examples did not present any difficulties in this regard.

4.4. A priori error analysis. Let us denote by $\mathcal{I}_h : [C(\bar{\Omega})]^2 \to [\mathcal{M}_h]^2$ the classical nodal interpolation operator with respect to a unisolvent set of Lagrangian interpolation nodes associated with the conforming space $\mathcal{M}_h$ and by $\mathcal{I}_\Gamma$ the restriction of $\mathcal{I}_h$ to the boundary nodes. By $\Pi_h^{\text{BDM}} \boldsymbol{u}$ we denote the BDM projection of $\boldsymbol{u}$, and $\Pi_h p$ is the L^2-projection of p onto $\mathcal{Q}_h$. Under adequate regularity assumptions, the following approximation properties hold (see [12, 28]):

$$(4.19) \quad \begin{aligned} \|\boldsymbol{u} - \Pi_h^{\text{BDM}} \boldsymbol{u}\|_{2,\mathcal{T}_h} &\leq C(\sqrt{\sigma} h^{k+1} + \sqrt{\nu_2} h^k) \|\boldsymbol{u}\|_{k+1,\Omega}, \\ \|\boldsymbol{y} - \mathcal{I}_h \boldsymbol{y}\|_{1,\Omega} &\leq C h^k \|\boldsymbol{y}\|_{k+1,\Omega}, \quad \|p - \Pi_h p\|_{0,\Omega} \leq C h^k \|p\|_{k,\Omega}. \end{aligned}$$

The following preliminary trace result can be proven as in [37, Lemma 4.3].

LEMMA 4.4. *Assume that $\boldsymbol{y}^{\mathrm{D}} \in [C(\bar{\Gamma})]^2$ and $\boldsymbol{y}_h^{\mathrm{D}} = \mathcal{I}_\Gamma \boldsymbol{y}^{\mathrm{D}}$. Then there is a lifting $\boldsymbol{y}_{h,1} \in \mathcal{M}_h$ such that $\boldsymbol{y}_{h,1}|_\Gamma = \boldsymbol{y}_h^{\mathrm{D}}$ and*

$$(4.20) \qquad \|\boldsymbol{y}_{h,1}\|_{1,\Omega} \le C_{\mathrm{lift}} \|\boldsymbol{y}_h^{\mathrm{D}}\|_{1/2,\Gamma},$$

where the constant $C_{\mathrm{lift}} > 0$ is independent of the mesh size.

Remark 2. If one assumes that $C_{\mathrm{dep}} C_{\mathrm{emb}} C_{\mathrm{lift}} \|\boldsymbol{y}_h^{\mathrm{D}}\|_{1/2,\Gamma} \le 1/2$ with C_{Lip}, C_{emb}, and C_{dep} defined by (4.20), (4.2), and (4.13), respectively, then, by Theorem 3.1, there exists a solution $(\boldsymbol{u}_h, \boldsymbol{y}_h)$ to (3.1) with $\boldsymbol{y}_h = \boldsymbol{y}_{h,0} + \boldsymbol{y}_{h,1}$ satisfying the stability bounds

$$(4.21) \qquad \|\boldsymbol{u}_h\|_{1,\mathcal{T}_h} \le \tilde{C}_{\boldsymbol{u}} C_{\mathrm{lift}} \|\boldsymbol{y}_h^{\mathrm{D}}\|_{1/2,\Gamma} \quad \text{and} \quad \|\boldsymbol{y}_h\|_{1,\mathcal{T}_h} \le \tilde{C}_{\boldsymbol{y}} C_{\mathrm{lift}} \|\boldsymbol{y}_h^{\mathrm{D}}\|_{1/2,\Gamma}.$$

If we assume additional regularity of the exact solution $\boldsymbol{y} \in [H^2(\Omega)]^2$, then $\|\boldsymbol{y}_h^{\mathrm{D}}\|_{1/2,\Gamma}$ is bounded independently of h (cf. [37, Lemma 4.7 and Remarks 4.8 and 4.9]).

THEOREM 4.2. *Let us consider liftings satisfying* (4.12), *and let us assume the data are sufficiently small* (4.13). *Let also $(\boldsymbol{u}, p, \boldsymbol{y})$, $(\boldsymbol{u}_h, p_h, \boldsymbol{y}_h)$ be the solutions of* (2.3) *and* (4.1), *respectively. Assume the condition*

$$(4.22) \qquad \max\{\|\boldsymbol{u}\|_{\boldsymbol{W}^{1,\infty}(\Omega)}, \|\boldsymbol{y}\|_{[L^\infty(\Omega)]^2}, \gamma_{\boldsymbol{F}}\} \le \min(M, \tilde{M})$$

with M sufficiently small as specified in (3.6), *and $\tilde{M}$ is bounded by the data of the problem in a way that will be made explicit in the proof. Furthermore, suppose that for $k = 1$, $\boldsymbol{u} \in \boldsymbol{C}^1(\bar{\Omega}) \cap \boldsymbol{H}^2(\Omega) \cap \boldsymbol{X}$, $p \in H^1(\Omega)$, and $\boldsymbol{y} \in [L^\infty(\Omega)]^2 \cap [H^2(\Omega)]^2$, and that for $k \ge 2$ there holds $\boldsymbol{u} \in \boldsymbol{H}^{k+1}(\Omega) \cap \boldsymbol{X}$, $p \in H^k(\Omega)$, and $\boldsymbol{y} \in [H^{k+1}(\Omega)]^2$. Then there exist constants $C > 0$ independent of the mesh size such that*

$$(4.23) \qquad \|\boldsymbol{u} - \boldsymbol{u}_h\|_{2,\mathcal{T}_h} + \|\boldsymbol{y} - \boldsymbol{y}_h\|_{1,\Omega} \le Ch^k (\|\boldsymbol{u}\|_{k+1,\Omega} + \|\boldsymbol{y}\|_{k+1,\Omega}),$$

$$(4.24) \qquad \|p - p_h\|_{0,\Omega} \le Ch^k (\|p\|_{k,\Omega} + \|\boldsymbol{u}\|_{k+1,\Omega} + \|\boldsymbol{y}\|_{k+1,\Omega}).$$

Proof. An application of integration by parts together with the assumed velocity regularity readily implies that the exact solution $(\boldsymbol{u}, p, \boldsymbol{y})$ satisfies

$$(4.25) \qquad a^h(\boldsymbol{y}; \boldsymbol{u}, \boldsymbol{v}_h) + c^h(\boldsymbol{u}; \boldsymbol{u}, \boldsymbol{v}_h) - b(\boldsymbol{v}_h, p) - d(\boldsymbol{y}, \boldsymbol{v}_h) = 0 \quad \text{for all } \boldsymbol{v}_h \in \boldsymbol{V}_h$$

(see, for example, [28, Lemma 3.1]). We then write a discrete analogue of (4.25) and subtract the result, leading to the following Galerkin orthogonality:

$$(4.26) \qquad \begin{aligned} a^h(\boldsymbol{y}; \boldsymbol{u}, \boldsymbol{v}_h) - a^h(\boldsymbol{y}_h; \boldsymbol{u}_h, \boldsymbol{v}_h) + c^h(\boldsymbol{u}; \boldsymbol{u}, \boldsymbol{v}_h) - c^h(\boldsymbol{u}_h; \boldsymbol{u}_h, \boldsymbol{v}_h) \\ - b(\boldsymbol{v}_h, p - p_h) - d(\boldsymbol{y} - \boldsymbol{y}_h, \boldsymbol{v}_h) = 0. \end{aligned}$$

In addition, it is not difficult to verify that

$$(4.27) \qquad b(\boldsymbol{u} - \boldsymbol{u}_h, q_h) = 0, \quad a_{\boldsymbol{y}}(\boldsymbol{y} - \boldsymbol{y}_h, \boldsymbol{\varphi}_h) + c_{\boldsymbol{y}}(\boldsymbol{u}, \boldsymbol{y}, \boldsymbol{\varphi}_h) - c_{\boldsymbol{y}}(\boldsymbol{u}_h, \boldsymbol{y}_h, \boldsymbol{\varphi}_h) = 0$$

for all $(q_h, \boldsymbol{\varphi}_h) \in \mathcal{Q}_h \times \mathcal{M}_{h,0}$. Let us define the errors

$$\begin{aligned} e_{\boldsymbol{u}} &:= (\boldsymbol{u} - \Pi_h^{\mathrm{BDM}} \boldsymbol{u}) + (\Pi_h^{\mathrm{BDM}} \boldsymbol{u} - \boldsymbol{u}_h) = \hat{e}_{\boldsymbol{u}} + \tilde{e}_{\boldsymbol{u}}, \\ e_p &:= (p - \Pi_h p) + (\Pi_h p - p_h) = \hat{e}_p + \tilde{e}_p, \\ e_{\boldsymbol{y}} &:= (\boldsymbol{y} - \mathcal{I}_h \boldsymbol{y}) + (\mathcal{I}_h \boldsymbol{y} - \boldsymbol{y}_h) = \hat{e}_{\boldsymbol{y}} + \tilde{e}_{\boldsymbol{y}}, \end{aligned}$$

so after testing (4.26) against $\boldsymbol{v}_h = \tilde{e}_{\boldsymbol{u}}$ and rearranging terms we end up with

$$
\begin{aligned}
& a^h(\boldsymbol{y}_h, \tilde{e}_{\boldsymbol{u}}, \tilde{e}_{\boldsymbol{u}}) + c^h(\boldsymbol{u}_h, \tilde{e}_{\boldsymbol{u}}, \tilde{e}_{\boldsymbol{u}}) = I_0 + I_1 + I_2, \quad \text{where} \\
& I_0 := d(\boldsymbol{y}, \tilde{e}_{\boldsymbol{u}}) - d(\boldsymbol{y}_h, \tilde{e}_{\boldsymbol{u}}), \\
(4.28) \quad & I_1 := [a^h(\boldsymbol{y}_h, \boldsymbol{u}, \tilde{e}_{\boldsymbol{u}}) - a^h(\mathcal{I}_h\,\boldsymbol{y}; \boldsymbol{u}, \tilde{e}_{\boldsymbol{u}})] \\
& \qquad\quad + [a^h(\mathcal{I}_h\,\boldsymbol{y}; \boldsymbol{u}, \tilde{e}_{\boldsymbol{u}}) - a^h(\boldsymbol{y}; \boldsymbol{u}, \tilde{e}_{\boldsymbol{u}})] - a^h(\boldsymbol{y}_h; \hat{e}_{\boldsymbol{u}}, \tilde{e}_{\boldsymbol{u}}), \\
& I_2 := [c^h(\boldsymbol{u}_h; \boldsymbol{u}, \tilde{e}_{\boldsymbol{u}}) - c^h(\Pi_h^{\mathrm{BDM}}\,\boldsymbol{u}; \boldsymbol{u}, \tilde{e}_{\boldsymbol{u}})] \\
& \qquad\quad + [c^h(\Pi_h^{\mathrm{BDM}}\,\boldsymbol{u}; \boldsymbol{u}, \tilde{e}_{\boldsymbol{u}}) - c^h(\boldsymbol{u}; \boldsymbol{u}, \tilde{e}_{\boldsymbol{u}})] - c^h(\boldsymbol{u}_h; \hat{e}_{\boldsymbol{u}}, \tilde{e}_{\boldsymbol{u}}).
\end{aligned}
$$

The rest of the proof will be devoted to finding appropriate bounds for these terms. Starting with I_0, we combine (2.2) and the triangular inequality to get

$$
I_0 \le \gamma_{\boldsymbol{F}} \|\boldsymbol{y} - \boldsymbol{y}_h\|_{1,\Omega} \|\tilde{e}_{\boldsymbol{u}}\|_{1,\mathcal{T}_h} \le \gamma_{\boldsymbol{F}} \big(\|\tilde{e}_{\boldsymbol{y}}\|_{1,\Omega} + \|\hat{e}_{\boldsymbol{y}}\|_{1,\Omega}\big) \|\tilde{e}_{\boldsymbol{u}}\|_{1,\mathcal{T}_h}.
$$

Next, from (4.5), the continuity of a^h, and the small data assumption in (4.22) we get

$$
I_1 \le \tilde{C}_{\mathrm{Lip}} \gamma_\nu \tilde{M} \big(\|\tilde{e}_{\boldsymbol{y}}\|_{1,\Omega} \|\tilde{e}_{\boldsymbol{u}}\|_{1,\mathcal{T}_h} + \|\hat{e}_{\boldsymbol{y}}\|_{1,\Omega} \|\tilde{e}_{\boldsymbol{u}}\|_{1,\mathcal{T}_h}\big) + \tilde{C}_a \|\hat{e}_{\boldsymbol{u}}\|_{1,\mathcal{T}_h} \|\tilde{e}_{\boldsymbol{u}}\|_{1,\mathcal{T}_h}.
$$

Moreover, from (4.6), (4.6), (2.9), (4.21), and again assumption (4.22), we obtain

$$
\begin{aligned}
I_2 & \le \tilde{C}_v \|\tilde{e}_{\boldsymbol{u}}\|_{1,\mathcal{T}_h}^2 \|\boldsymbol{u}\|_{1,\Omega} + \tilde{C}_v \|\hat{e}_{\boldsymbol{u}}\|_{1,\mathcal{T}_h} \|\boldsymbol{u}\|_{1,\mathcal{T}_h} \|\tilde{e}_{\boldsymbol{u}}\|_{1,\mathcal{T}_h} + \tilde{C}_v \|\boldsymbol{u}_h\|_{1,\mathcal{T}_h} \|\hat{e}_{\boldsymbol{u}}\|_{1,\mathcal{T}_h} \|\tilde{e}_{\boldsymbol{u}}\|_{1,\mathcal{T}_h} \\
& \le \tilde{C}_v C_\infty \tilde{M} \big(\|\tilde{e}_{\boldsymbol{u}}\|_{1,\mathcal{T}_h}^2 + \|\hat{e}_{\boldsymbol{u}}\|_{1,\mathcal{T}_h} \|\tilde{e}_{\boldsymbol{u}}\|_{1,\mathcal{T}_h}\big) + \tilde{C}_v \tilde{C}_{\boldsymbol{u}} C_{\mathrm{lift}} \|\boldsymbol{y}_h^{\mathrm{D}}\|_{1/2,\Gamma} \|\hat{e}_{\boldsymbol{u}}\|_{1,\mathcal{T}_h} \|\tilde{e}_{\boldsymbol{u}}\|_{1,\mathcal{T}_h}.
\end{aligned}
$$

Inserting the bounds on I_0, I_1, and I_2 into (4.28), and also using the coercivity of the left-hand side, thanks to (4.7)–(4.8) and applying Young's inequality we arrive at

$$
\begin{aligned}
(4.29) \quad \tilde{\alpha}_a \|\tilde{e}_{\boldsymbol{u}}\|_{1,\mathcal{T}_h}^2 & \le \big((1 + C_{\mathrm{Lip}})\tilde{M}\|\hat{e}_{\boldsymbol{y}}\|_{1,\Omega} + (\tilde{C}_a + \tilde{C}_v \tilde{C}_{\boldsymbol{u}} \|\boldsymbol{y}_h^{\mathrm{D}}\|_{H^{1/2}(\Gamma)}) \|\hat{e}_{\boldsymbol{u}}\|_{1,\mathcal{T}_h}\big) \|\tilde{e}_{\boldsymbol{u}}\|_{1,\mathcal{T}_h} \\
& \quad + \left(\tilde{M}\left(\frac{1 + \tilde{C}_{\mathrm{Lip}} \gamma_\nu}{2} + \tilde{C}_v C_\infty\right)\right) \|\tilde{e}_{\boldsymbol{u}}\|_{1,\mathcal{T}_h}^2 + \frac{1 + \tilde{C}_{\mathrm{Lip}} \gamma_\nu}{2} \tilde{M} \|\tilde{e}_{\boldsymbol{y}}\|_{1,\mathcal{T}_h}^2.
\end{aligned}
$$

We handle (4.27) in a similar way and take $\boldsymbol{\varphi}_h = \tilde{e}_{\boldsymbol{y}}$ as the test function. This leads to

$$
\begin{aligned}
a_{\boldsymbol{y}}(\tilde{e}_{\boldsymbol{y}}, \tilde{e}_{\boldsymbol{y}}) + c_{\boldsymbol{y}}(\boldsymbol{y}_h; \boldsymbol{y}_h, \tilde{e}_{\boldsymbol{y}}) & = -a_{\boldsymbol{y}}(\hat{e}_{\boldsymbol{y}}, \tilde{e}_{\boldsymbol{y}}) - c_{\boldsymbol{y}}(\tilde{e}_{\boldsymbol{u}}; \boldsymbol{y}, \tilde{e}_{\boldsymbol{y}}) \\
& \quad - c_{\boldsymbol{y}}(\hat{e}_{\boldsymbol{u}}; \boldsymbol{y}, \tilde{e}_{\boldsymbol{y}}) - c_{\boldsymbol{y}}(\boldsymbol{u}_h; \hat{e}_{\boldsymbol{y}}, \tilde{e}_{\boldsymbol{y}}).
\end{aligned}
$$

In addition, on the left-hand side we use the coercivity of $a_{\boldsymbol{y}}$, properties (2.8), (4.4b), (4.21), the embedding (2.9), as well as assumption (4.22) to get

$$
\begin{aligned}
\hat{\alpha}_a \|\tilde{e}_{\boldsymbol{y}}\|_{1,\Omega}^2 & \le \hat{C}_a \|\hat{e}_{\boldsymbol{y}}\|_{1,\Omega} \|\tilde{e}_{\boldsymbol{y}}\|_{1,\Omega} + \tilde{C}_1 C_\infty \tilde{M} \big(\|\tilde{e}_{\boldsymbol{u}}\|_{1,\mathcal{T}_h} \|\tilde{e}_{\boldsymbol{y}}\|_{1,\Omega} + \|\hat{e}_{\boldsymbol{u}}\|_{1,\mathcal{T}_h} \|\tilde{e}_{\boldsymbol{y}}\|_{1,\Omega}\big) \\
& \quad + \tilde{C}_1 \tilde{C}_v C_{\mathrm{lift}} \|\boldsymbol{y}_h^{\mathrm{D}}\|_{1/2,\Gamma} \|\hat{e}_{\boldsymbol{y}}\|_{1,\Omega} \|\tilde{e}_{\boldsymbol{y}}\|_{1,\Omega},
\end{aligned}
$$

and after applying Young's inequality and regrouping terms, we have

$$
\begin{aligned}
(4.30) \quad \hat{\alpha}_a \|\tilde{e}_{\boldsymbol{y}}\|_{1,\Omega}^2 & \le \big((\hat{C}_a + \tilde{C}_1 \tilde{C}_{\boldsymbol{u}} C_{\mathrm{lift}} \|\boldsymbol{y}_h^{\mathrm{D}}\|_{1/2,\Gamma}) \|\hat{e}_{\boldsymbol{y}}\|_{1,\Omega} + \tilde{C}_1 C_\infty \tilde{M} \|\hat{e}_{\boldsymbol{u}}\|_{1,\mathcal{T}_h}\big) \|\tilde{e}_{\boldsymbol{y}}\|_{1,\Omega} \\
& \quad + \frac{1}{2} \tilde{C}_1 C_\infty \tilde{M} \big(\|\tilde{e}_{\boldsymbol{u}}\|_{1,\mathcal{T}_h}^2 + \|\tilde{e}_{\boldsymbol{y}}\|_{1,\Omega}^2\big).
\end{aligned}
$$

Adding (4.29) and (4.30) and defining $\check{C} := (1 + \tilde{C}_{\mathrm{Lip}}\gamma_\nu + \tilde{C}_1 C_\infty)/2$ we obtain

$$(\tilde{\alpha}_a - \tilde{M}(\check{C} + \tilde{C}_v C_\infty))\|\tilde{e}_{\boldsymbol{u}}\|_{1,\mathcal{T}_h}^2 + (\hat{\alpha}_a - \tilde{M}\check{C})\|\tilde{e}_{\boldsymbol{y}}\|_{1,\Omega}^2$$
$$\leq C\big(\|\hat{e}_{\boldsymbol{y}}\|_{1,\Omega} + \|\hat{e}_{\boldsymbol{u}}\|_{1,\mathcal{T}_h}\big)\big(\|\tilde{e}_{\boldsymbol{u}}\|_{1,\mathcal{T}_h} + \|\tilde{e}_{\boldsymbol{y}}\|_{1,\mathcal{T}_h}\big).$$

Hence, if we choose $\tilde{M}$ such that $\tilde{M} < \min\{\tilde{\alpha}_a/(\check{C} + \tilde{C}_v C_\infty), \hat{\alpha}_a/\check{C}\}$ (note that this constant depends only on the data of the problem), then we readily obtain $\|\tilde{e}_{\boldsymbol{u}}\|_{1,\mathcal{T}_h} + \|\tilde{e}_{\boldsymbol{y}}\|_{1,\Omega} \leq C(\|\hat{e}_{\boldsymbol{y}}\|_{1,\Omega} + \|\hat{e}_{\boldsymbol{u}}\|_{1,\mathcal{T}_h})$. Using now the approximation properties in (4.19), we straightforwardly get (4.23).

For the pressure estimate we consider the discrete inf-sup condition (4.10) as well as (4.3c). It follows that

$$\|\tilde{e}_p\|_{0,\Omega} \leq \frac{1}{\tilde{\beta}} \sup_{\boldsymbol{v}_h \in \boldsymbol{V}_h\setminus\{\boldsymbol{0}\}} \frac{b(\boldsymbol{v}_h, \tilde{e}_p)}{\|\boldsymbol{v}_h\|_{1,\mathcal{T}_h}} \leq \frac{1}{\tilde{\beta}} \sup_{\boldsymbol{v}_h \in \boldsymbol{V}_h\setminus\{\boldsymbol{0}\}} \frac{b(\boldsymbol{v}_h, e_p)}{\|\boldsymbol{v}_h\|_{1,\mathcal{T}_h}} + \frac{1}{\tilde{\beta}} \sup_{\boldsymbol{v}_h \in \boldsymbol{V}_h\setminus\{\boldsymbol{0}\}} \frac{b(\boldsymbol{v}_h, \hat{e}_p)}{\|\boldsymbol{v}_h\|_{1,\mathcal{T}_h}}$$

$$(4.31) \qquad \leq \frac{1}{\tilde{\beta}} \sup_{\boldsymbol{v}_h \in \boldsymbol{V}_h\setminus\{\boldsymbol{0}\}} \frac{b(\boldsymbol{v}_h, e_p)}{\|\boldsymbol{v}_h\|_{1,\mathcal{T}_h}} + \frac{1}{\tilde{\beta}}\|\hat{e}_p\|_{0,\Omega}.$$

Now for any $\boldsymbol{v}_h \in \boldsymbol{V}_h$, (4.26) implies the bound $b(\boldsymbol{v}_h, e_p) \leq I_3 + I_4 + I_5$, where

$$I_3 = \big|d(\boldsymbol{y}, \boldsymbol{v}_h) - d(\boldsymbol{y}_h, \boldsymbol{v}_h)\big|,$$
$$I_4 = \big|a^h(\boldsymbol{y}; \boldsymbol{u}, \boldsymbol{v}_h) - a^h(\boldsymbol{y}_h; \boldsymbol{u}, \boldsymbol{v}_h)\big| + \big|a^h(\boldsymbol{y}_h, e_{\boldsymbol{u}}, \boldsymbol{v}_h)\big|,$$
$$I_5 = \big|c^h(\boldsymbol{u}; \boldsymbol{u}, \boldsymbol{v}_h) - c^h(\boldsymbol{u}_h; \boldsymbol{u}, \boldsymbol{v}_h)\big| + \big|c^h(\boldsymbol{u}_h; e_{\boldsymbol{u}}, \boldsymbol{v}_h)\big|.$$

Hence we can use property (2.2) to deduce that $I_3 \leq \gamma_{\boldsymbol{F}}\|e_{\boldsymbol{y}}\|_{1,\Omega}\|\boldsymbol{v}_h\|_{1,\mathcal{T}_h}$. From (4.5), (4.3a), and assumption (4.22), it then follows that

$$I_4 \leq \tilde{C}_{\mathrm{Lip}}\gamma_\nu\|e_{\boldsymbol{y}}\|_{1,\Omega}\|\boldsymbol{u}\|_{\boldsymbol{W}^{1,\infty}(\Omega)}\|\boldsymbol{v}_h\|_{1,\mathcal{T}_h} + C\|e_{\boldsymbol{u}}\|_{2,\mathcal{T}_h}\|\boldsymbol{v}_h\|_{1,\mathcal{T}_h},$$
$$\leq \tilde{C}_{\mathrm{Lip}}\gamma_\nu\tilde{M}\|e_{\boldsymbol{y}}\|_{1,\Omega}\|\boldsymbol{v}_h\|_{1,\mathcal{T}_h} + C\|e_{\boldsymbol{u}}\|_{2,\mathcal{T}_h}\|\boldsymbol{v}_h\|_{1,\mathcal{T}_h}.$$

Now we use (4.6), (2.9), (4.21), and the bound in (4.6) to get

$$I_5 \leq \tilde{C}_v\|\boldsymbol{u}_h\|_{1,\mathcal{T}_h}\|e_{\boldsymbol{u}}\|_{1,\mathcal{T}_h}\|\boldsymbol{v}_h\|_{1,\mathcal{T}_h} + \tilde{C}_v\|\boldsymbol{u}\|_{1,\mathcal{T}_h}\|e_{\boldsymbol{u}}\|_{1,\mathcal{T}_h}\|\boldsymbol{v}_h\|_{1,\mathcal{T}_h}$$
$$\leq \tilde{C}_v C_\infty \tilde{M}\|e_{\boldsymbol{u}}\|_{2,\mathcal{T}_h}\|\boldsymbol{v}_h\|_{1,\mathcal{T}_h} + \tilde{C}_v \tilde{C}_{\boldsymbol{u}} C_{\mathrm{lift}}\|\boldsymbol{y}_h^{\mathrm{D}}\|_{H^{1/2}(\Gamma)}\|e_{\boldsymbol{u}}\|_{2,\mathcal{T}_h}\|\boldsymbol{v}_h\|_{1,\mathcal{T}_h}.$$

The estimates on I_3, I_4, and I_5 therefore yield

$$(4.32) \qquad \big|b(\boldsymbol{v}_h, e_p)\big| \leq C\big(\|e_{\boldsymbol{y}}\|_{1,\Omega} + \|e_{\boldsymbol{u}}\|_{2,\mathcal{T}_h}\big)\|\boldsymbol{v}_h\|_{1,\mathcal{T}_h}.$$

Hence (4.24) follows by replacing (4.32) in (4.31) and using the approximation properties (4.19). □

Notice that, thanks to the divergence-free property of the discrete velocities, the bound (4.23) confirms that the family of methods proposed here is pressure robust (see also the discussion in [26]). This can be also observed numerically, for instance in Table 3 where the magnitude of the pressure errors does not affect the magnitude of the velocity errors.

5. Numerical tests. The following set of examples provides numerical confirmation of the convergence rates anticipated in Theorem 4.2. We further validate the proposed method by comparing our produced results against benchmark solutions found in the literature, and we present one test oriented to applications inherent to doubly diffusive flows in porous media. The linearization of the system of equations associated with the assembled form of (4.1) is carried out by Newton's method, setting a relative tolerance of 1E-8 on the residuals. In turn, the solution of the resulting linear systems present at each Newton step is conducted using the biconjugate gradient stabilized Krylov solver (BiCGStab). In the implementation of the method, the normal component of the velocity is fixed in the form of an essential boundary condition, whereas its tangential component is incorporated as a natural boundary condition and imposed *à la* Nitsche (see, e.g., [24]). Moreover, the condition of zero mean value for the pressure approximation is implemented using a real Lagrange multiplier. All tests were implemented using the open-source finite element library FEniCS [4].

5.1. Example 1: Accuracy test. In our first computational test we examine the convergence of the Galerkin method (4.1), taking as computational domain the square $\Omega = (-1, 1)^2$, and considering a sequence of uniformly refined meshes $\{\mathcal{T}_{h,l}\}_l$ of mesh size $h_l = 2^{-l}\sqrt{2}$. We take a buoyancy term of the form $\boldsymbol{F}(\boldsymbol{y}) = (T + N_r S)\boldsymbol{g}$, where N_r is the solutal to the thermal buoyancy ratio, and choose an exponential form for the viscosity $\nu(T) = \nu_2 \exp(-T)$, $\boldsymbol{g} = (0, 1)^T$, $\boldsymbol{K}^{-1} = \sigma \boldsymbol{I}$, $\boldsymbol{D} = 1000\boldsymbol{I}$, $a_0 = \sqrt{\sigma}10^k$. Following the approach of manufactured solutions, we prescribe boundary data and additional external forces and adequate source terms so that the closed-form solutions to (1.1) are given by the smooth functions

$$\boldsymbol{u}(x, y) = \big(\sin(\pi x)\cos(\pi y), -\cos(\pi x)\sin(\pi y)\big)^{\mathrm{T}}, \quad p(x, y) = \cos(\pi x)\exp(y),$$
$$T(x, y) = 0.5 + 0.5\cos(xy), \quad S(x, y) = 0.1 + 0.3\exp(xy).$$

Relative errors in their natural norms, along with the corresponding convergence rates computed as

$$\mathsf{e}_{\boldsymbol{u}} = \|\boldsymbol{u} - \boldsymbol{u}_h\|_{1,\mathcal{T}_h}/\|\boldsymbol{u}\|_{1,\mathcal{T}_h}, \quad \mathsf{e}_p = \|p - p_h\|_{0,\Omega}/\|p\|_{0,\Omega}, \quad \mathsf{e}_T = \|T - T_h\|_{1,\Omega}/\|T\|_{1,\Omega},$$
$$\mathsf{e}_S = \|S - S_h\|_{1,\Omega}/\|S\|_{1,\Omega}, \quad \mathtt{rate} = \log(e_{(\cdot)}/\tilde{e}_{(\cdot)})[\log(h/\tilde{h})]^{-1},$$

where $e, \tilde{e}$ denote errors generated on two consecutive meshes of sizes h and $\tilde{h}$, respectively, are listed in Table 1 for $k = 1, 2$, where the model constants are chosen as stated above. We can observe that the total error is dominated by the pressure approximation, and that the discrete velocities are divergence free. The tabulated values also indicate an optimal $\mathcal{O}(h^k)$ convergence, consistently with the theoretical bounds stated in Theorem 4.2. We also conduct two additional series of accuracy tests focusing on the cases where the viscosity and permeability coefficients scale differently, changing from Stokes to Darcy regimes. These values are collected in Tables 2 and 3, respectively. Apart from an increase of the pressure error, we can see that the experimental rates of convergence remain close to the optimal behavior.

TABLE 1

Example 1 (accuracy test): Experimental errors and convergence rates for the approximate solutions $\boldsymbol{u}_h$, p_h, T_h, and S_h, and the ℓ^∞-norm of the vector formed by the divergence of the discrete velocity computed for each discretization. Values are displayed for the first and second order schemes for a flow regime with $\nu_2 = \sigma = 1$.

k	DoF	$\mathbf{e}_{\boldsymbol{u}}$	rate	$\mathbf{e}_p$	rate	$\mathbf{e}_T$	rate	$\mathbf{e}_S$	rate	$\|\mathrm{div}\,\boldsymbol{u}_h\|_{\infty,\Omega}$
1	195	0.6798	–	1.5670	–	0.3498	–	0.2721	–	1.33E-15
	707	0.3779	0.847	1.1370	0.563	0.1975	0.824	0.1385	0.974	4.88E-15
	2691	0.1873	1.012	0.6614	0.787	0.1019	0.954	0.0696	0.992	9.77E-15
	10499	0.0923	1.021	0.3485	0.925	0.0513	0.988	0.0348	0.998	2.13E-14
	41475	0.0459	1.007	0.1771	0.977	0.0257	0.997	0.0174	0.999	4.62E-14
2	523	0.3258	1.657	1.7741	1.243	0.1221	1.101	0.0338	1.767	9.03E-14
	1971	0.0847	1.943	0.6826	1.378	0.0326	1.905	0.0089	1.928	2.23E-13
	7651	0.0179	2.237	0.2159	1.661	0.0083	1.968	0.0023	1.979	4.82E-13
	30147	0.0038	2.238	0.0587	1.877	0.0021	1.991	0.0006	1.994	9.96E-13
	119683	0.0008	2.108	0.0151	1.964	0.0005	1.998	0.0001	1.998	2.01E-12

TABLE 2

Example 1 (accuracy test): Errors and convergence rates under a Stokes regime with $\nu_2 = 10, \sigma = 0$.

k	DoF	$\mathbf{e}_{\boldsymbol{u}}$	rate	$\mathbf{e}_p$	rate	$\mathbf{e}_T$	rate	$\mathbf{e}_S$	rate	$\|\mathrm{div}\,\boldsymbol{u}_h\|_{\infty,\Omega}$
1	195	2.1490	–	14.352	–	0.3498	–	0.2721	–	1.55E-15
	707	1.2041	0.835	10.710	0.429	0.1975	0.824	0.1385	0.974	4.00E-15
	2691	0.5958	1.015	6.3981	0.749	0.1019	0.954	0.0696	0.992	8.88E-15
	10499	0.2925	1.026	3.4170	0.904	0.0513	0.988	0.0348	0.998	2.31E-14
	41475	0.1453	1.010	1.7461	0.968	0.0257	0.997	0.0174	1.000	4.26E-14
2	523	1.0380	1.652	17.152	1.119	0.1221	1.101	0.0338	1.767	9.24E-14
	1971	0.2688	1.949	6.7861	1.338	0.0326	1.905	0.0089	1.928	2.29E-13
	7651	0.0568	2.241	2.1562	1.654	0.0083	1.968	0.0023	1.979	4.87E-13
	30147	0.0121	2.239	0.5875	1.876	0.0021	1.991	0.0006	1.994	1.01E-12
	119683	0.0028	2.108	0.1507	1.963	0.0005	1.998	0.0001	1.998	2.00E-12

TABLE 3

*Example 1 (accuracy test): Errors and convergence rates for the approximate solutions for a Darcy regime, with $\nu_2 = 1, \sigma = 10000$.*

k	DoF	$\mathbf{e}_{\boldsymbol{u}}$	rate	$\mathbf{e}_p$	rate	$\mathbf{e}_T$	rate	$\mathbf{e}_S$	rate	$\|\mathrm{div}\,\boldsymbol{u}_h\|_{\infty,\Omega}$
1	195	5.3102	–	287.42	–	0.3498	–	0.2721	–	1.78E-15
	707	1.6182	1.715	148.01	0.958	0.1975	0.825	0.1385	0.974	4.44E-15
	2691	0.4303	1.911	72.992	1.021	0.1019	0.954	0.0696	0.993	1.07E-14
	10499	0.1324	1.701	36.721	0.991	0.0514	0.988	0.0348	0.998	2.13E-14
	41475	0.0516	1.359	18.472	0.992	0.0257	0.997	0.0174	1.000	4.26E-14
2	523	1.9250	2.483	270.41	2.175	0.1221	1.101	0.0338	1.767	9.49E-14
	1971	0.5142	1.905	51.930	2.38	0.0326	1.905	0.0089	1.928	2.27E-13
	7651	0.1364	1.914	11.504	2.175	0.0083	1.968	0.0023	1.979	4.94E-13
	30147	0.0389	1.808	3.1610	1.863	0.0021	1.991	0.0006	1.994	9.99E-13
	119683	0.0104	1.900	1.0190	1.633	0.0005	1.998	0.0001	1.998	2.03E-12

5.2. Example 2: Soret and Dufour effects in a porous cavity. Using the following dimensionless variables, $x = x^*/H, y = y^*/X, \boldsymbol{u} = \boldsymbol{u}H/\nu, p = p^*H/\rho\nu, T = (T^* - T_0)/(T_1 - T_0)$, and $C = (C^* - c_0)/(C_1 - C_0)$ (where H is the cavity height and ν the kinematic viscosity of the fluid), we can write the equations describing transport

TABLE 4

Example 2 *(porous cavity): (left) Sketched domain with boundary conditions; (right) comparison of average Nusselt and Sherwood numbers for* $N = 0$, Le $= 10$ *with thermal Rayleigh numbers on Darcy's regime.*
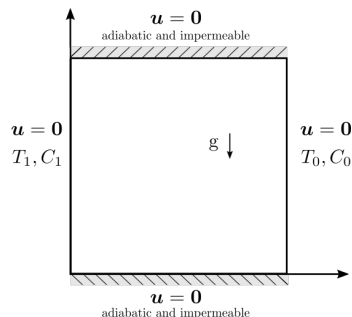
Ra		100	200	400	1000	2000
Nu	Present study	3.10	4.97	7.84	13.72	20.31
	Ref. [14]	3.15	5.02	7.83	14.01	20.00
	Ref. [22]	3.11	4.96	7.77	13.47	19.90
Sh	Present study	13.58	20.73	30.91	49.42	66.80
	Ref. [14]	13.54	20.11	27.96	48.01	71.25
	Ref. [22]	13.25	19.86	28.41	48.32	69.29

phenomena in a square porous cavity with thermal and concentration diffusion in the form (1.1). We set $\boldsymbol{K} = \mathrm{Da}\,\boldsymbol{I}$, $\nu(T) = 1$, and $\boldsymbol{F}(\boldsymbol{y}) = (\mathrm{Gr}_T\, T + \mathrm{Gr}_C\, C)\boldsymbol{g}$, where $\boldsymbol{g} = (0, -1)^{\mathrm{T}}$ points in the direction of gravity, $\boldsymbol{y} = (T, C)^{\mathrm{T}}$, and the diffusion coefficients are given by

$$\boldsymbol{D} = \begin{bmatrix} R_k/\mathrm{Pr} & \mathrm{Du} \\ \mathrm{Sr} & 1/\mathrm{Sc} \end{bmatrix}.$$

Here, R_k is the thermal conductivity ratio, $\mathrm{Gr}_T, \mathrm{Gr}_C$ are the thermal and solutal Grashof numbers respectively, $\mathrm{Da} = \kappa/H^2$ is the Darcy number, $\mathrm{Pr} = \nu/\alpha$ the Prandtl number, $\mathrm{Sc} = \nu/D_C$ the Schmidt number, and the ratio $\mathrm{Le} = \mathrm{Sc}/\mathrm{Pr}$ the Lewis number.

For a preliminary validation we conduct a series of computational tests using a buoyancy ratio $N := \mathrm{Gr}_C/\mathrm{Gr}_T = 0$. The computational domain is the unit square $\Omega := (0, 1)^2$, considering no-slip velocity conditions on Γ. Temperature and concentration are kept at T_0, C_0 and T_1, C_1 at the right and left walls, respectively, where $T_0 < T_1$ and $C_0 < C_1$. Horizontal walls are adiabatic and impermeable, as depicted on the left of Table 4. In this subsection we will use $k = 2$ and a mesh with 20000 elements. We compute Nusselt and Sherwood numbers and compare these outputs against well-known benchmark data from [14] and [22]. The average values of Nu and Sh values on the left vertical wall are, respectively,

$$\mathrm{Nu} = \int_0^1 \frac{\partial T}{\partial x}\bigg|_{x=0} \mathrm{d}y, \quad \mathrm{Sh} = \int_0^1 \frac{\partial C}{\partial x}\bigg|_{x=0} \mathrm{d}y.$$

For the values $R_k = 1.0$, $\mathrm{Da} = 10^{-7}$, $\mathrm{Le} = 10$, $\mathrm{Sr} = 0$, $\mathrm{Du} = 0$, and $\mathrm{Pr} = 10$, results for different thermal Rayleigh values are computed and summarized on the right panel of Table 4 along with the results from [14, 22]. For $\mathrm{Ra} \leq 1000$, the values of Nu and Sh are within a relative error of 3%, for the last value $\mathrm{Ra} = 2000$, within 6%.

Keeping the remaining parameters fixed, we now set $\mathrm{Ra} = 100$, $\mathrm{Le} = 0.8$, and $N = 1$. The effect of Dufour parameter on the flow, thermal, and concentration fields are portrayed in Figure 1 for $\mathrm{Du} \in \{0.1, 1\}$. The velocity field and isotherms are in qualitative agreement with those in [10, Figure 2]. In Figure 2 we repeat
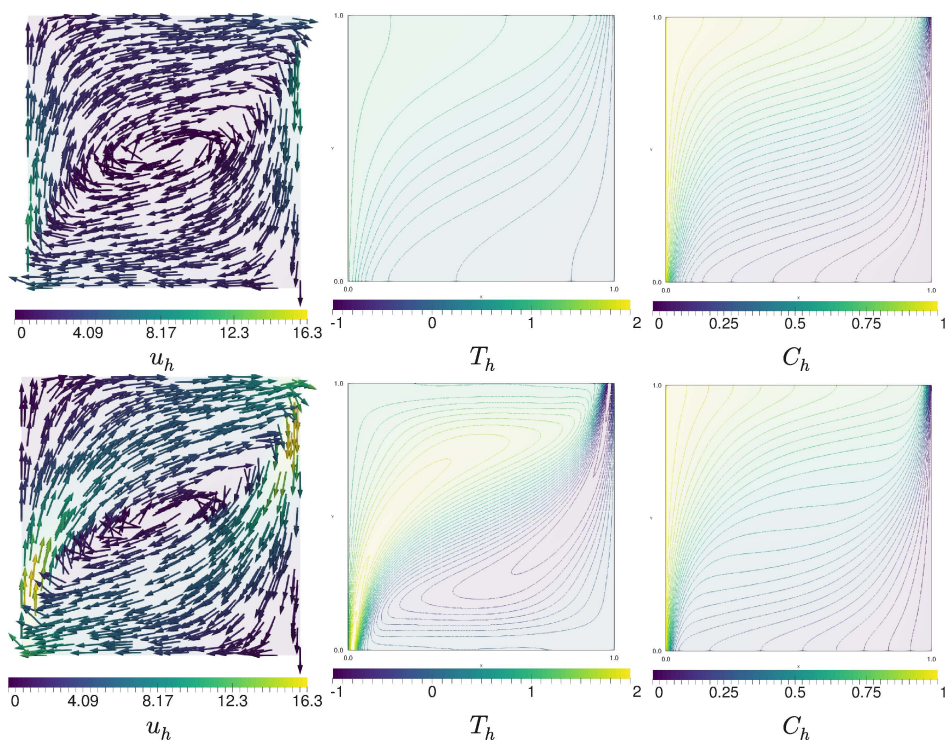
FIG. 1. *Example 2 (porous cavity): (left) Velocity field, (middle) isotherms, and (right) concentration contours for (top)* Du = 0.1, *(bottom)* Du = 1.
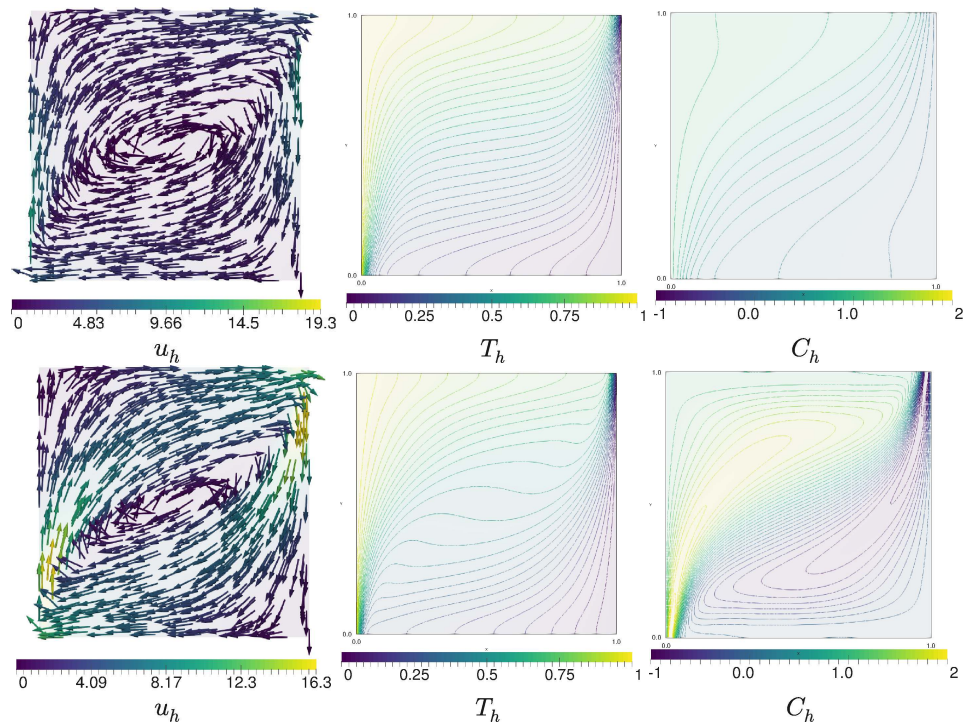

FIG. 2. *Example 2 (porous cavity): (left) Velocity field, (middle) isotherms, and (right) concentration contours for (top)* Sr = 0.1, *(bottom)* Sr = 1.
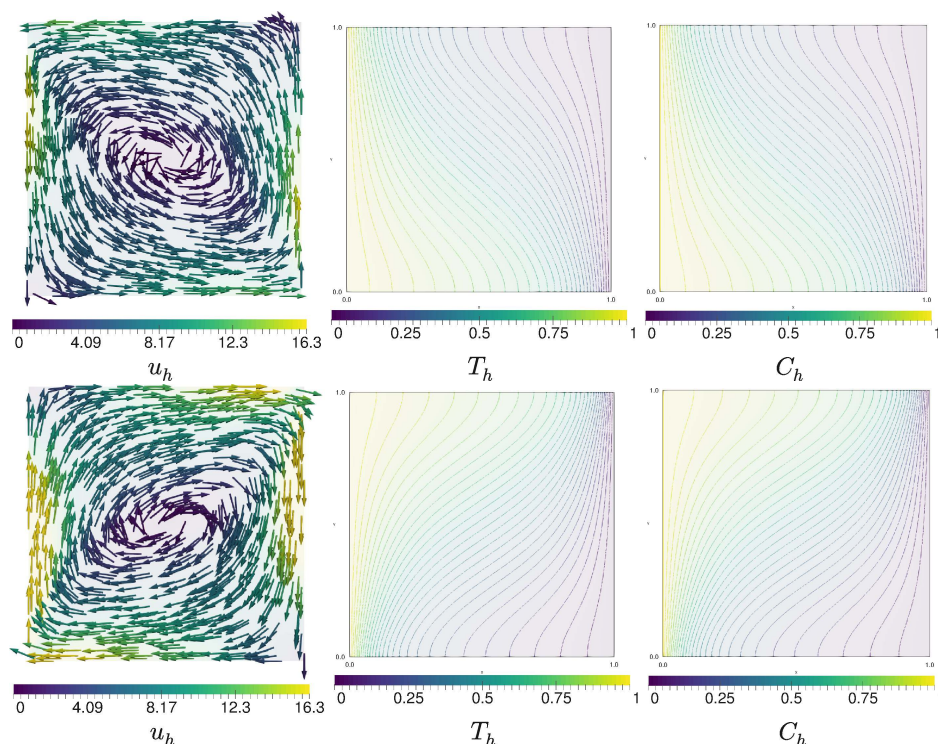
FIG. 3. *Example 2 (porous cavity): (left) Velocity field, (middle) isotherms, and (right) concentration contours for (top) $N = -5$, (bottom) $N = 5$.*

the plots keeping Du $= 0$ and with Soret values of Sr $\in \{0.1, 1\}$. As expected, the result is almost symmetric with an exchange of behavior between temperature and concentration. Moreover, in both cases an increment of Sr or Du drives an increase of velocity in the recirculation patterns. Finally, in Figure 3 we fix Du $= 0.5$, Sr $= 0.5$ and test the effect of buoyancy by setting $N = -5$ and, alternatively, $N = 5$. We can see the reversion of flow direction caused by the difference in buoyancy of the species. Note that in the last case $\boldsymbol{D}$ is not positive definite and solvability of the coupled problem cannot be guaranteed. Nevertheless, convergence of the Newton iterations was observed for a broad range of parameters (Sr, Pr $\in [10^{-3}, 10^3]$, $N \in [1, 10]$, Da $\in [10^{-7}, 1]$, Ra $\in [100, 2000]$). The convergence of Newton iterates is lost only when the Soret number Sr takes values greater than 5 (and provided that $N \geq 0$ and Du $= 0$).

5.3. Example 3: Bioconvection of oxytactic bacteria. With the notation $\boldsymbol{y} = (c_1, c_2)^{\mathrm{T}}$ the oxytactic bacteria bioconvection phenomenon (see [30, 31]) can be modeled by (1.1), with diffusion, reaction, and remaining concentration-dependent coefficients given by

$$\boldsymbol{D}(\boldsymbol{y}) = \begin{bmatrix} D_1 & -\alpha r(c_2)c_1 \\ 0.0 & D_2 \end{bmatrix}, \quad g(\boldsymbol{y}) = \beta r(c_2) \begin{pmatrix} 0 \\ -1 \end{pmatrix}, \quad \boldsymbol{F}(\boldsymbol{y}) = \gamma c_1 \boldsymbol{g},$$

$$\boldsymbol{g} = \begin{pmatrix} 0 \\ -1 \end{pmatrix}, \quad r(c_2) = \frac{1}{2} \left(1 + \frac{c_2 - c_2^*}{\sqrt{(c_2 - c_2^*)^2 + \varepsilon^2}} \right).$$
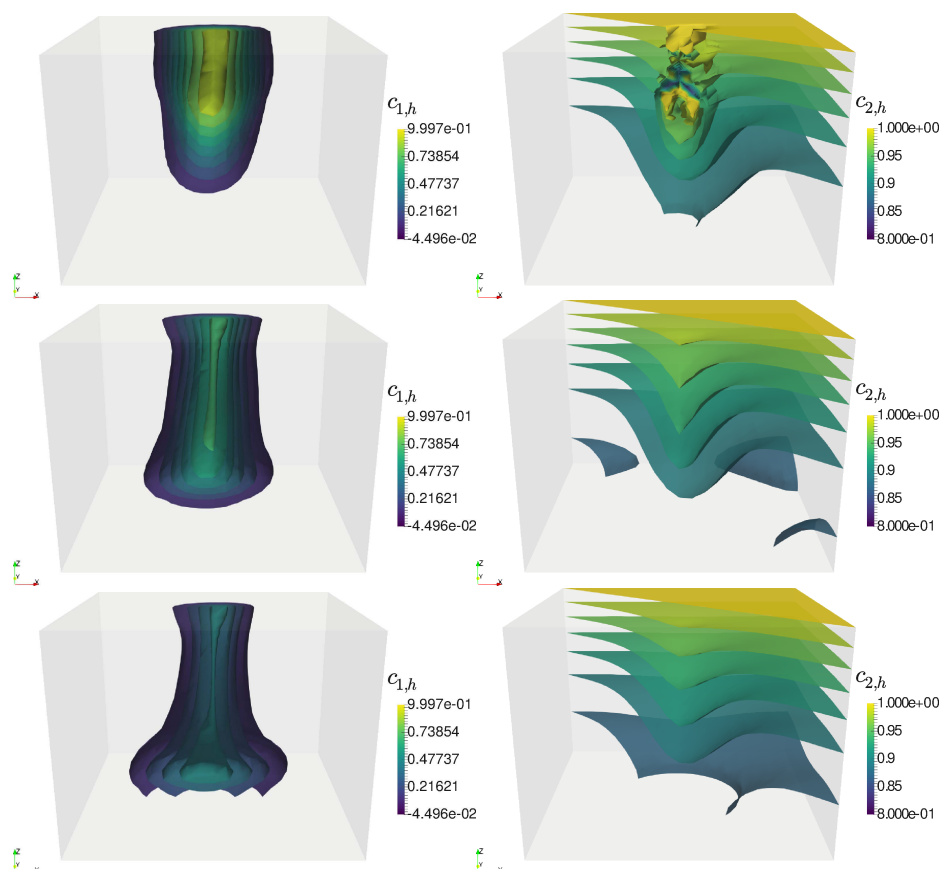
FIG. 4. *Example 3 (bioconvection): Patterns generated by the bacterial chemotaxis towards oxygen concentration. Snapshots of the obtained solutions at times (top) $t = 0.1$, (middle) $t = 0.3$, and (bottom) $t = 0.5$.*

We consider a rectangular prism with square base $[0, 1] \times [0, 1]$ and height 0.75, discretized into a tetrahedral mesh of 48000 cells. Fixing the parameters $\beta = 0.1$, $D_1 = 0.01$, $D_2 = 0.2$, $\gamma = 5000$, $\alpha = 0.25$, Sc $= 10^{-2}$, and $\mu = 2$, we use a pseudo-time-step, using $\Delta t = 0.1$ to compute intermediate state solutions, starting from a distribution of bacteria packed in a ball of radius 0.2 and placed near the top of the vessel. Snapshots (at advanced time) of the numerical solution are displayed in Figures 4 and 5. We observe how the bacteria propagate downwards, producing re-circulating zones as indicated by the velocity field. The first snapshot shows that the oxygen concentration has more variation on the top layers due to the competition between consumption of the high bacterial concentration, recirculating flow, and diffusion. Later on, oxygen concentration follows the flow direction, showing higher values downwards in the center of the recirculating zones. The pressure distributes from low on the top, to high on the bottom, also decreasing its magnitude as the bacteria reach the vessel's bottom.
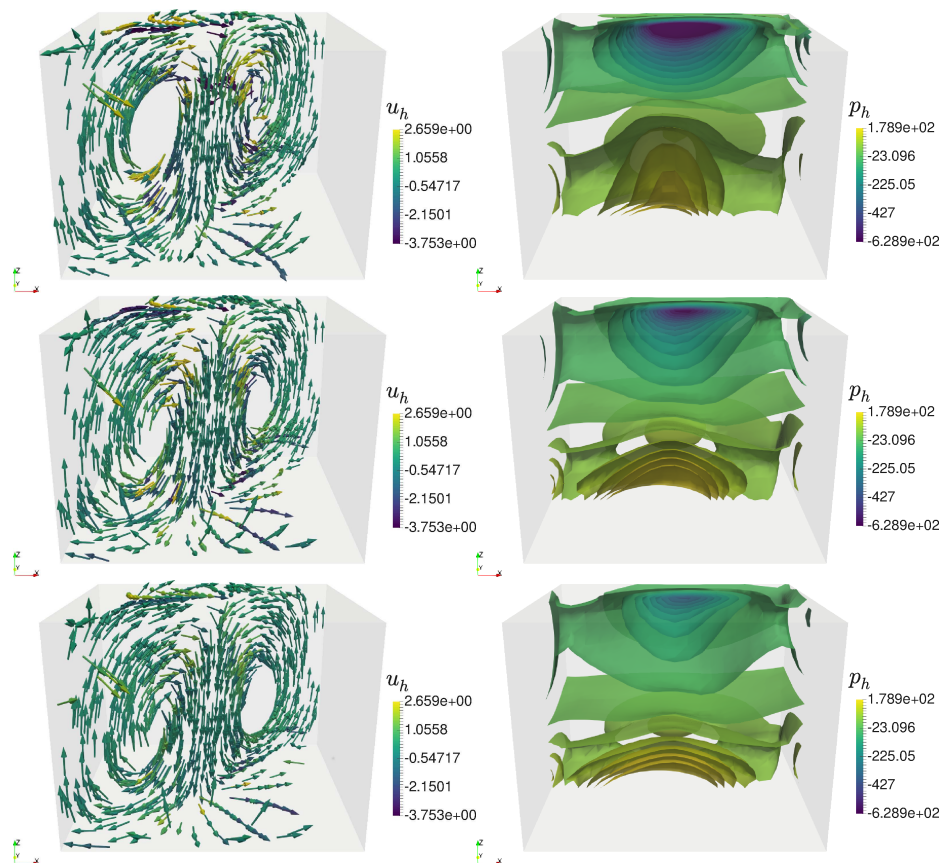
FIG. 5. *Example 3 (bioconvection): Patterns generated by the bacterial chemotaxis towards oxygen concentration. Snapshots of the obtained solutions at times (top)* $t = 0.1$*, (middle)* $t = 0.3$*, and (bottom)* $t = 0.5$*.*

REFERENCES

[1] A. AGOUZAL AND K. ALLALI, *Numerical analysis of reaction front propagation model under Boussinesq approximation*, Math. Methods Appl. Sci., 26 (2003), pp. 1529–1572.

[2] K. ALLALI, *A priori and a posteriori error estimates for Boussinesq equations*, Int. J. Numer. Anal. Model., 2 (2005), pp. 179–196.

[3] A. ALLENDES, G. BARRENECHEA, AND C. NARANJO, *A divergence-free low-order stabilized finite element method for a generalized steady state Boussinesq problem*, Comput. Methods Appl. Mech. Engrg., 340 (2018), pp. 90–120.

[4] M.S. ALNÆS, J. BLECHTA, J. HAKE, A. JOHANSSON, B. KEHLET, A. LOGG, C. RICHARDSON, J. RING, M.E. ROGNES, AND G.N. WELLS, *The FEniCS project version 1.5*, Arch. Numer. Softw., 3 (2015), pp. 9–23.

[5] M. ALVAREZ, G.N. GATICA, B. GOMEZ-VARGAS, AND R. RUIZ-BAIER, *New mixed finite element methods for natural convection with phase-change in porous media*, J. Sci. Comput., 80 (2019), pp. 141–174.

[6] M. ALVAREZ, G.N. GATICA, AND R. RUIZ-BAIER, *An augmented mixed-primal finite element method for a coupled flow-transport problem*, ESAIM Math. Model. Numer. Anal., 49 (2015), pp. 1399–1427.

[7] M. ALVAREZ, G.N. GATICA, AND R. RUIZ-BAIER, *A mixed-primal finite element approximation of a sedimentation-consolidation system*, Math. Models Methods Appl. Sci., 26 (2016), pp. 867–900.

[8]   V. ANAYA, M. BENDAHMANE, D. MORA, AND R. RUIZ-BAIER, *On a primal-mixed vorticity-based formulation for reaction-diffusion-Brinkman systems*, Netw. Heterog. Media, 13 (2018), pp. 69–94.

[9]   D.N. ARNOLD, F. BREZZI, B. COCKBURN, AND L.D. MARINI, *Unified analysis of discontinuous Galerkin methods for elliptic problems*, SIAM J. Numer. Anal., 39 (2002), pp. 1749–1779.

[10] C.S. BALLA AND K. NAIKOTI, *Soret and Dufour effects on free convective heat and solute transfer in fluid saturated inclined porous cavity*, Engrg. Sci. Technol., 18 (2015), pp. 543–554.

[11] F. BREZZI, J. DOUGLAS, AND L.D. MARINI, *Two families of mixed finite elements for second order elliptic problems*, Numer. Math., 47 (1985), pp. 217–235.

[12] F. BREZZI AND M. FORTIN, *Mixed and Hybrid Finite Element Methods*, Springer Ser. Comput. Math. 15, Springer, New York, 1991.

[13] R. BÜRGER, S.K. KENETTINKARA, R. RUIZ-BAIER, AND H. TORRES, *Coupling of discontinuous Galerkin schemes for viscous flow in porous media with adsorption*, SIAM J. Sci. Comput., 40 (2018), pp. B637–B662.

[14] A. ÇIBIK AND S. KAYA, *Finite element analysis of a projection-based stabilization method for the Darcy-Brinkman equations in double-diffusive convection*, Appl. Numer. Math., 64 (2013), pp. 35–49.

[15] B. COCKBURN, G. KANSCHAT, AND D. SCHÖTZAU, *A locally conservative LDG method for the incompressible Navier-Stokes equations*, Math. Comput., 74 (2005), pp. 1067–1095.

[16] E. COLMENARES, G.N. GATICA, AND R. OYARZÚA, *Fixed point strategies for mixed variational formulations of the stationary Boussinesq problem*, C. R. Math. Acad. Sci. Paris Ser. I, 354 (2016), pp. 57–62.

[17] X. CUI, *The regularity criterion for weak solutions to the n-dimensional Boussinesq system*, Bound. Value Probl., 2017 (2017), 44.

[18] R. DE AGUIAR, B. CLIMENT-EZQUERRA, M.A. ROJAS-MEDAR, AND M.D. ROJAS-MEDAR, *On the convergence of Galerkin spectral methods for a bioconvective flow*, J. Math. Fluid Mech., 19 (2017), pp. 91–104.

[19] D.A. DI PIETRO AND A. ERN, *Mathematical Aspects of Discontinuous Galerkin Methods*, Series Math. Appl. (Berlin) 69, Springer, Berlin, 2011.

[20] V. GIRAULT AND P.A. RAVIART, *Finite Element Methods for Navier-Stokes Equations. Theory and Algorithms*, Springer, Berlin, 1986.

[21] V. GIRAULT, B. RIVIÈRE, AND M.F. WHEELER, *A discontinuous Galerkin method with nonoverlapping domain decomposition for the Stokes and Navier-Stokes problems*, Math. Comput., 74 (2005), pp. 53–84.

[22] B. GOYEAU, J.P. SONGBE, AND D. GOBIN, *Numerical study of double-diffusive natural convection in a porous cavity using the Darcy-Brinkman formulation*, Int. J. Heat Mass Transf., 39 (1996), pp. 1363–1378.

[23] J. GUO AND P.N. KALONI, *Double diffusive convection in a porous medium, nonlinear stability and the Brinkman effect*, Stud. Appl. Math., 94 (1995), pp. 341–358.

[24] P. HANSBO AND M.G. LARSON, *Discontinuous Galerkin methods for incompressible and nearly incompressible elasticity by Nitsche's method*, Comput. Methods Appl. Mech. Engrg., 191 (2002), pp. 1895–1908.

[25] J.C. HEINRICH, *A finite element model for double diffusion convection*. Internat. J. Numer. Methods Engrg., 20 (1984), pp. 447–464.

[26] V. JOHN, A. LINKE, C. MERDON, M. NEILAN, AND L.G. REBHOLZ, *On the divergence constraint in mixed finite element methods for incompressible flows*. SIAM Rev., 59 (2017), pp. 492–544.

[27] O.A. KARAKASHIAN AND W.N. JUREIDINI, *A nonconforming finite element method for the stationary Navier–Stokes equations*, SIAM J. Numer. Anal., 35 (1998), pp. 93–120.

[28] J. KÖNNÖ AND R. STENBERG, *H(div)-conforming finite elements for the Brinkman problem*, Math. Models Methods Appl. Sci., 21 (2011), pp. 2227–2248.

[29] I. KUKAVICA, F. WANG, AND M. ZIANE, *Persistence of regularity for solutions of the Boussinesq equations in Sobolev spaces*, Adv. Differential Equations, 21 (2016), pp. 85–108.

[30] H.G. LEE AND J. KIM, *Numerical investigation of falling bacterial plumes caused by bioconvection in a three-dimensional chamber*, Eur. J. Mech. B Fluids, 52 (2015), pp. 120–130.

[31] P. LENARDA, M. PAGGI, AND R. RUIZ-BAIER, *Partitioned coupling of advection-diffusion-reaction systems and Brinkman flows*, J. Comput. Phys., 344 (2017), pp. 281–302.

[32] C. LIN AND L.E. PAYNE, *Continuous dependence on the Soret coefficient for double diffusive convection in Darcy flow*, J. Math. Anal. Appl., 342 (2008), pp. 311–325.

[33] S.A. LORCA AND J.L. BOLDRINI, *Stationary solutions for generalized Boussinesq models*, J. Differential Equations, 124 (1996), pp. 389–406.

[34] S.A. Lorca and J.L. Boldrini, *The initial value problem for a generalized Boussinesq model*, Nonlinear Anal., 36 (1999), pp. 457–480.

[35] E. Magyari and A. Postelnicu, *Double-diffusive natural convection flows with thermosolutal symmetry in porous media in the presence of Soret–Dufour effects*, Transp. Porous Media, 88 (2011), pp. 149–167.

[36] P. Nithiarasu, K.N. Seetharamu, and T. Sundararajan, *Double-diffusive natural convection in an enclosure filled with fluid-saturated porous medium: A generalized non-Darcy approach*, Numer. Heat Transf. Part A, 30 (1996), pp. 413–426.

[37] R. Oyarzúa, T. Qin, and D. Schötzau, *An exactly divergence-free finite element method for a generalized Boussinesq problem*, IMA J. Numer. Anal., 34 (2014), pp. 1104–1135.

[38] R. Oyarzúa and M. Serón, *A Divergence-Conforming DG-Mixed Finite Element Method for the Stationary Boussinesq Problem*, Technical report 2018-21, CI^{2}MA, Universidad de Concepción, Concepción, Chile, http://www.ci2ma.udec.cl (2018).

[39] P.R. Patil and C.P. Parvathy, *Thermohaline convection with cross-diffusion in an anisotropic porous medium*, Proc. Indian Acad. Sci. Math. Sci., 99 (1989), pp. 93–101.

[40] J.N. Shadid, R.S. Tuminaro, and H.F. Walker, *An inexact Newton method for fully coupled solution of the Navier-Stokes equations with heat and mass transport*, J. Comput. Phys., 137 (1997), pp. 155–185.

[41] Q. Shao, M. Fahs, A. Younes, A. Makradi, and T. Mara, *A new benchmark reference solution for double-diffusive convection in a heterogeneous porous medium*, Numer. Heat Transf. Part B, 70 (2016), pp. 373–392.

[42] L.Q. Tang and T.T.H. Tsang, *A least-squares finite element method for doubly-diffusive convection*, Int. J. Comput. Fluid Dyn., 3 (1994), pp. 1–17.

[43] R. Temam, *Navier-Stokes equations. Theory and Numerical Analysis*, AMS-Chelsea Ser., Providence, RI, 2001.

[44] J. Woodfield, M. Alvarez, B. Gomez-Vargas, and R. Ruiz-Baier, *Stability and finite element approximation of phase change models for natural convection in porous media*, J. Comput. Appl. Math., 360 (2019), pp. 117–137.

[45] N. Zabaras and D. Samanta, *A stabilized volume-averaging finite element method for flow in porous media and binary alloy solidification processes*, Internat. J. Numer. Methods Engrg., 60 (2004), pp. 1103–1138.

[46] Y.J. Zhuang, H.Z. Yu, and Q.Y. Zhu, *A thermal non-equilibrium model for 3D double diffusive convection of power-law fluids with chemical reaction in the porous medium*, Int. J. Heat Mass Transf., 115 (2017), pp. 670–694.